Four-Coordinate Molybdenum Chalcogenide Complexes Relevant to Nitrous Oxide N−N Bond Cleavage by Three-Coordinate Molybdenum(III): Synthesis, Characterization, Reactivity, and Thermochemistry

Adam R. Johnson,[†] William M. Davis,[†] Christopher C. Cummins,*[,†] Scafford Serron,[‡] Steven P. Nolan,*[,‡] Djamaladdin G. Musaev,*[,§] and Keiji Morokuma[§]

Contribution from the Department of Chemistry Room 2-227, Massachusetts Institute of Technology, Cambridge, Massachusetts 02139-4307, Department of Chemistry, University of New Orleans, New Orleans, Louisiana 70148, Cherry L. Emerson Center for Scientific Computation and Department of Chemistry, Emory University, Atlanta, Georgia 30322

Received May 8, 1997

Abstract: The terminal chalcogenide complexes Mo(E)(N[R]Ar)$_3$ (R = C(CD$_3$)$_2$CH$_3$, Ar = 3,5-C$_6$H$_3$Me$_2$), where E = O, S, Se, and Te, were prepared by reaction of the three-coordinate complex Mo(N[R]Ar)$_3$ with ONC$_5$H$_5$, S$_8$ or SC$_2$H$_4$, Se, and Te/PEt$_3$ in respective yields of 72, 63, 80, and 73%. The Mo(E)(N[R]Ar)$_3$ complexes were studied by EPR, SQUID, cyclic voltammetry, ^{2}H NMR spectroscopy, and single-crystal X-ray diffraction. Thermolysis of each Mo(E)(N[R]Ar)$_3$ complex resulted in (formal) *tert*-butyl radical elimination giving molybdenum(VI) chalcogenide complexes Mo(E)(NAr)(N[R]Ar)$_2$ in yields of 85 (E = O), 84 (E = S), 64 (E = Se) and 40% (E = Te). *tert*-Butyl elimination kinetics were monitored (^{2}H NMR) over a 62−104 °C temperature range for Mo(O)(N[R]Ar)$_3$, and from 66 to 93 °C for Mo(S)(N[R]Ar)$_3$; in both cases, a first-order decay was observed. Treatment of Mo(O)(N[R]Ar)$_3$ with iodine (0.5 equiv) provided [Mo(O)(N[R]Ar)$_3$][I] in 88% yield. The triflate salt [Mo(O)(N[R]Ar)$_3$][O$_3$SCF$_3$] was prepared similarly (71% yield) upon treatment of Mo(O)(N[R]Ar)$_3$ with [Cp$_2$Fe][O$_3$SCF$_3$]. Small-scale experiments monitored by ^{1}H NMR spectroscopy established that Mo(N[R]Ar)$_3$ deoxygenates OSMe$_2$, NO$_2$, and SO$_2$ but fails to deoxygenate CO$_2$. Also essentially inert to Mo(N[R]Ar)$_3$ were found to be OPPh$_3$, *t*-BuNCO, and O$_2$SMe$_2$. Treatment of Mo(N[R]Ar)$_3$ with Se$_2$Ph$_2$ provided Mo(SePh)(N[R]Ar)$_3$ in 72% yield. Treatment of Mo(N[R]Ar)$_3$ with CS$_2$ led to Mo(S)(N[R]Ar)$_3$ and (μ-CS)[Mo(N[R]Ar)$_3$]$_2$; the latter was isolated in 42% yield and was the subject of an X-ray diffraction study. Bond dissociation enthalpies *D*(MoE) for Mo(E)(N[R]Ar)$_3$ (E = O and S) were experimentally determined to be 155.6 ± 1.6 and 104.4 ± 1.2 kcal mol^{-1}, respectively. MoE bond lengths predicted by density functional B3LYP calculations (lanl2dz + d$_E$ basis set) for the model complexes Mo(E)(NH$_2$)$_3$ (E = O, S, Se, and Te) were found to compare favorably with the experimentally determined MoE bond lengths. Predicted bond dissociation enthalpies *D*(MoE) for the hypothetical complexes Mo(E)(NH$_2$)$_3$ are 91 (E = Se) and 71 (E = Te) kcal mol^{-1}. A key finding is that Mo(N[R]Ar)$_3$ *selectively* splits the nitrous oxide N−N bond to give Mo(N)(N[R]Ar)$_3$ and Mo(NO)(N[R]Ar)$_3$, despite the fact that the oxo complex Mo(O)(N[R]Ar)$_3$ possesses a very strong Mo−O bond and can be prepared by an alternate route.

1. Introduction

It was shown recently that Mo(N[R]Ar)$_3$ (R = C(CD$_3$)$_2$CH$_3$, Ar = 3,5-C$_6$H$_3$Me$_2$) is a monomeric species containing trigonal-planar molybdenum(III).[1,2] The elemental pnictogens dinitrogen and white phosphorus react readily with Mo(N[R]Ar)$_3$ to give, respectively, Mo(N)(N[R]Ar)$_3$ and Mo(P)(N[R]Ar)$_3$ *via* dramatic reductive cleavage reactions.[2−4] The latter are diamagnetic pseudotetrahedral molybdenum(VI) compounds possessing molybdenum−pnictogen triple bonds, the strength of which is thought to provide a thermodynamic driving force for the reductive cleavage reactions.

Surprising selectivity for nitrogen over oxygen was observed[1] in the reaction of Mo(N[R]Ar)$_3$ with nitrous oxide, a reaction found to proceed according to equation eq 1:

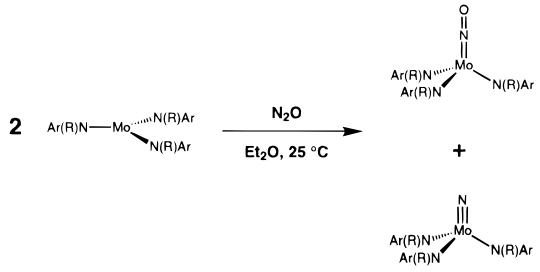

(1)

Such selectivity is exceedingly unusual for reactions involving nitrous oxide, in that N$_2$O typically donates an oxygen atom to

[†] Massachusetts Institute of Technology.
[‡] University of New Orleans.
[§] Emory University.

(1) Laplaza, C. E.; Odom, A. L.; Davis, W. M.; Cummins, C. C.; Protasiewicz, J. D. *J. Am. Chem. Soc.* **1995**, *117*, 4999.
(2) Laplaza, C. E.; Johnson, M. J. A.; Peters, J. C.; Odom, A. L.; Kim, E.; Cummins, C. C.; George, G. N.; Pickering, I. J. *J. Am. Chem. Soc.* **1996**, *118*, 8623.
(3) Laplaza, C. E.; Cummins, C. C. *Science* **1995**, *268*, 861.
(4) Laplaza, C. E.; Davis, W. M.; Cummins, C. C. *Angew. Chem., Int. Ed. Engl.* **1995**, *34*, 2042.

S0002-7863(97)01491-1 CCC: $15.00
Published on Web 02/20/1998

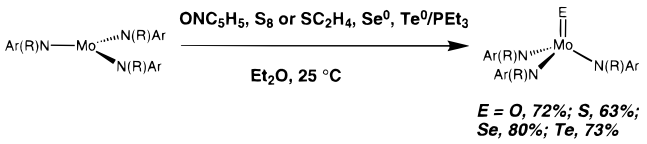

Figure 1. Synthetic protocol for the four Mo(E)(N[R]Ar$_3$ complexes.

reducing agents, thereby liberating dinitrogen.[5−7] The nitrous oxide NN bond is ca. 75 kcal mol^{-1} stronger than its NO bond, a fact underscoring a thermodynamic bias for NO bond activation in reactions of nitrous oxide.[8] One might therefore have predicted the reaction between Mo(N[R]Ar)$_3$ and nitrous oxide to occur according to eq 2:

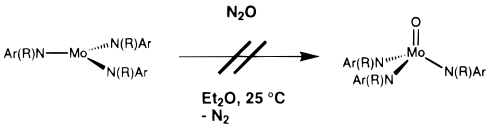

(2)

If for some reason the unknown oxomolybdenum(V) species Mo(O)(N[R]Ar)$_3$ were inherently thermodynamically unstable, this might explain the observed selectivity (e.g., eq 1 as opposed to eq 2). To explore this possibility we set out to synthesize Mo(O)(N[R]Ar)$_3$ by an independent route. This paper reports on the synthesis, structure, and properties of Mo(O)(N[R]Ar)$_3$, which was synthesized successfully by reaction of Mo(N[R]-Ar)$_3$ with pyridine *N*-oxide (see Figure 1). In this context, and as displayed in Figure 1, syntheses of the other chalcogenide compounds Mo(E)(N[R]Ar)$_3$ (E = S, Se, and Te) were developed based on reactions of Mo(N[R]Ar)$_3$ with the respective elemental chalcogen.

For the Mo(E)(N[R]Ar)$_3$ (E = O and S) complexes, the reaction chemistry proved amenable to calorimetry experiments, such that the heat of reaction of Mo(N[R]Ar)$_3$ with pyridine *N*-oxide and ethylene sulfide could be determined. As described in Section 2.1.8, the numbers so derived can be related to the Mo═E (E = O and S) bond dissociation enthalpies. Since for E = Se and Te the reaction chemistry was not amenable to calorimetry, the Mo═E bond dissociation enthalpies for these species have been estimated *via* a density functional theory study of the four Mo(E)(N[R]Ar)$_3$ complexes.

Consequently, the series of molybdenum(V) chalcogenide complexes (Mo(E)(N[R]Ar)$_3$; E = O, S, Se, and Te) have been investigated intensively with regard to their chemical and physical properties, one outcome of which is the finding that they are subject to thermal N−C bond homolysis (Section 2.3). This unusual reaction provided a series of chalcogenide−imide complexes Mo(E)(NAr)(N[R]Ar)$_2$ (E = O, S, Se, and Te) bearing molybdenum in its highest oxidation state.

Rounding out the present study of molybdenum chalcogenide complexes derived from Mo(N[R]Ar)$_3$ are a series of reactions involving interaction of Mo(N[R]Ar)$_3$ with various chalcogen-containing compounds. These include activation and bond cleavage reactions of nitrogen and sulfur dioxides that occur in homogeneous solution but are reminiscent of dissociative adsorption of these species on metal surfaces. It is observed that while some small molecules react with Mo(N[R]Ar)$_3$ readily under mild conditions, some, such as carbon dioxide, react only slowly or not at all.

2. Results and Discussion

2.1. Synthesis and Characterization of Mo(E)(N[R]Ar)$_3$ (E = O, S, Se, and Te). 2.1.1. Synthesis. Figure 1 displays the synthetic methods used and typical yields obtained in the preparation of the dark-colored Mo(E)(N[R]Ar)$_3$ complexes. A noteworthy observation is that while the Mo(E)(N[R]Ar)$_3$ complexes (E = S, Se, and Te) were preparable by direct reaction of Mo(N[R]Ar)$_3$ with the elemental chalcogen (with triethylphosphine catalysis in the case of Mo(Te)(N[R]Ar)$_3$), Mo(O)(N[R]Ar)$_3$ was not obtained from reactions of Mo(N[R]-Ar)$_3$ with O_2, pyridine *N*-oxide being used instead to effect the desired transformation. Reactions of Mo(N[R]Ar)$_3$ with dioxygen led to complex mixtures. The reaction of Mo(N[R]-Ar)$_3$ with ethylene sulfide was found, not surprisingly, to constitute an alternate synthetic route to Mo(S)(N[R]Ar)$_3$. In a control experiment for the synthesis of Mo(Te)(N[R]Ar)$_3$, it was determined that Mo(N[R]Ar)$_3$ does not give any observable reaction with PEt_3. No intermediate complexes were observed in any of the reactions leading to the Mo(E)(N[R]Ar)$_3$ complexes.

Transition-metal complexes possessing terminal Se or Te ligands are fairly rare but have been the subject of several recent papers.[9] Such complexes fall into the more general class of species containing terminal multiple bonds involving the heavier group 15 or 16 elements, species which are currently attracting a fair amount of attention as synthetic targets.[10]

2.1.2. NMR Data. ^{2}H NMR spectroscopy[11] was used to assay conversion of Mo(N[R]Ar)$_3$ to the Mo(E)(N[R]Ar)$_3$ complexes, the former exhibiting a single peak at 64 ppm[1] and the latter each exhibiting a peak of approximate line width 30 Hz near 7 ppm. In principle, one would expect two methyl and two aryl environments to be reflected in the proton NMR spectra of Mo(E)(N[R]Ar)$_3$, but in each case only two signals (assigned to the two methyl environments) were located. Signals for the aryl protons of d[1] Mo(E)(N[R]Ar)$_3$ were presumably broadened into the base line.

2.1.3. Infrared Data. Of interest in characterizing the Mo(E)(N[R]Ar)$_3$ complexes are the bands attributable to Mo═E stretching vibrations. The solution spectra of Mo(E)(N[R]Ar)$_3$ exhibited bands at 893, 492, 342, and 286 cm^{-1}, which are so assigned for E = O, S, Se, and Te, respectively. Confirmation of the assignments was made by digital subtraction of the Mo(O)(N[R]Ar)$_3$ spectrum from the Mo(S)(N[R]Ar)$_3$ spectrum and by subtraction of the Mo(Se)(N[R]Ar)$_3$ spectrum from the Mo(Te)(N[R]Ar)$_3$ spectrum.

By way of comparison, the $[Mo(E)_4]^{2-}$ ions exhibit bands at 897, 458, and 255 cm^{-1} for E = O, S, and Se, respectively.[12] No literature values of molybdenum−tellurium stretching frequencies were found for comparison with the data for Mo(Te)(N[R]Ar)$_3$. Christou and Arnold have described a

(5) Vaughan, G. A.; Sofield, C. D.; Hillhouse, G. L.; Rheingold, A. L. *J. Am. Chem. Soc.* **1989**, *111*, 5491.
(6) Matsunaga, P. T.; Hillhouse, G. L.; Rheingold, A. L. *J. Am. Chem. Soc.* **1993**, *115*, 2075.
(7) Bottomley, F. *Polyhedron* **1992**, *11*, 1707.
(8) Hintz, P. A.; Sowa, M. B.; Ruatta, S. A.; Anderson, S. L. *J. Chem. Phys.* **1991**, *94*, 6446.
(9) Siemeling, U. *Angew. Chem., Int. Ed. Engl.* **1993**, *32*, 67. Christou, V.; Arnold, J. *Angew. Chem., Int. Ed. Engl.* **1993**, *32*, 1450. Gerlach, C. P.; Arnold, J. *Inorg. Chem.* **1996**, *35*, 5770. Cummins, C. C.; Schrock, R. R.; Davis, W. M. *Inorg. Chem.* **1994**, *33*, 1448. Howard, W. A.; Parkin, G. *J. Am. Chem. Soc.* **1994**, *116*, 606. Murphy, V. J.; Parkin, G. J. *Am. Chem. Soc.* **1995**, *117*, 3522.
(10) Scheer, M. *Angew. Chem., Int. Ed. Engl.* **1995**, *34*, 1997.
(11) Johnson, A.; Everett, G. W., Jr. *J. Am. Chem. Soc.* **1972**, *94*, 1419. Wheeler, W. D.; Kaizaki, S.; Legg, J. *I. Inorg. Chem.* **1982**, *21*, 3248. Li, Z.; Goff, H. M. *Inorg. Chem.* **1992**, *31*, 1547.
(12) Müller, A.; Diemann, E.; Jostes, R.; Bögge, H. *Angew. Chem., Int. Ed. Engl.* **1981**, *20*, 934.

terminal telluride complex for which the metal−tellurium stretching vibration is 460 cm^{-1}.[9]

2.1.4. Magnetic Susceptibility. Variable-temperature SQUID magnetometry measurements of the magnetic susceptibility were made for solid $Mo(E)(N[R]Ar)_3$, yielding μ_{eff} values of 1.66, 1.63, 1.75, and 1.86 μ_B for E = O, S, Se, and Te, respectively. These data have been corrected for all temperature-independent contributions to the susceptibility, including diamagnetism and temperature-independent paramagnetism, by including an appropriate parameter in the least-squares fit of susceptibility versus temperature to the Curie−Weiss law. In all four cases, exceedingly good fits were obtained. Values of θ obtained from the fits ranged between −1 and −5 K. The only point of interest here is that the magnetic behavior of $Mo(E)(N[R]Ar)_3$ is consistent with their formulation as mononuclear complexes of molybdenum(V).

Solution susceptibility measurements for $Mo(E)(N[R]Ar)_3$ made at room temperature yielded values of μ_{eff} close to 2.1 μ_B. Here, corrections for diamagnetism were made using Pascal's constants but no attempt was made to correct for temperature-independent paramagnetism. The SQUID data are thus deemed more indicative of the true magnetic-moment value for the $Mo(E)(N[R]Ar)_3$ complexes.

2.1.5. EPR Spectra. A progression is noted in the frozen-glass EPR spectra of $Mo(E)(N[R]Ar)_3$ such that while $Mo(Te)(N[R]Ar)_3$ and $Mo(Se)(N[R]Ar)_3$ are clearly rhombic systems, with three well-resolved *g* values, the spectra for $Mo(S)(N[R]Ar)_3$ and $Mo(O)(N[R]Ar)_3$ are less well-resolved. In all four cases, computer fitting of the observed EPR spectra indicated the systems to be rhombic. In each case observed *g* values were in the window between 1.85 and 2.2. Interestingly, the isotropic hyperfine coupling constants to molybdenum, being on the order of 20−35 Gauss, were seen to decrease in the order E = O, S, Se, Te. The latter finding is interpreted in terms of increasing covalency in the M−E π-bond on going from E = O to E = Te, consistent with theoretical results presented below.

As described below, the orbital containing the unpaired electron in $Mo(E)(N[R]Ar)_3$ is thought to possess substantial Mo−E π-antibonding character. If $Mo(E)(N[R]Ar)_3$ were to possess 3-fold symmetry about the Mo−E bond, then the SOMO would be doubly-degenerate, a Jahn−Teller-unstable situation. That complexes $Mo(E)(N[R]Ar)_3$ prefer to adopt structures of symmetry lower than C_3 is consistent with their rhombic EPR spectra and the X-ray crystallographic data presented below.

2.1.6. X-ray Crystallography. An ORTEP diagram of $Mo(O)(N[R]Ar)_3$ is displayed in Figure 2. Salient bond distances and angles are given in the figure caption. The molybdenum−oxygen distance of 1.706(2) Å in $Mo(O)(N[R]Ar)_3$ is somewhat long for a molybdenum(V) oxo complex, though not outside of the usual range.[13] The other bond distances are typical, although the arrangement of the three N(R)Ar ligands is of unusually low symmetry, with no pseudo-3-fold axis and no pseudo mirror plane evident. In fact, the molecule is somewhere in-between the two limiting symmetries C_3 and C_s. The O−Mo−N−C_{tert} dihedral angles are 40°, 3°, and 62°, whereas a typical value is 35° for 3-fold symmetric d^0 $M(X)(N[R]Ar)_3$ complexes.[2] The N[R]Ar ligand exhibiting the 62° O−Mo−N−C_{tert} dihedral angle is slightly pyramidalized at nitrogen, the sum of the angles about the N atom being 356.2°. Planarity is observed at the other two nitrogens, as is typical of the transition-metal dihydrocarbylamido functionality.[14] Although the three N(R)Ar ligands in $Mo(O)(N[R]Ar)_3$ are quite

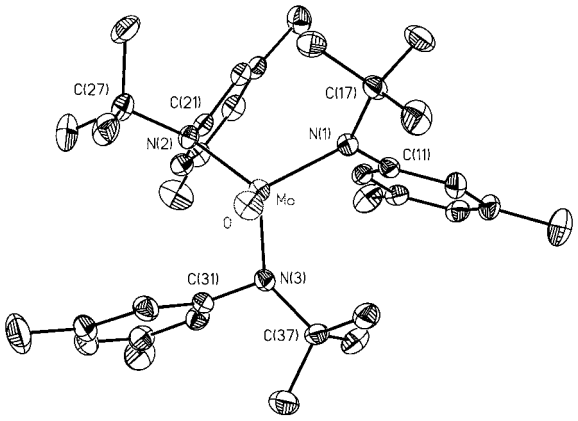

Figure 2. Structural drawing of $Mo(O)(N[R]Ar)_3$ with thermal ellipsoids at the 35% probability level. Selected bond lengths (Å): Mo−O, 1.706(2); Mo−N(3), 1.973(2); Mo−N(2), 1.980(2); Mo−N(1), 1.990(2). Selected bond angles (deg): O−Mo−N(3), 103.22(10); O−Mo−N(2), 115.53(10); N(3)−Mo−N(2), 111.60(9); O−Mo−N(1), 108.56(10); N(3)−Mo−N(1), 108.50(9); N(2)−Mo−N(1), 109.13(10).

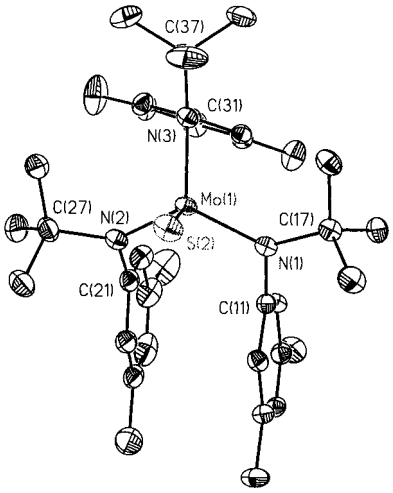

Figure 3. Structural drawing of $Mo(s)(N[R]Ar)_3$ with thermal ellipsoids at the 35% probability level. Selected bond lengths (Å): Mo(1)−N(2), 1.947(4); Mo(1)−N(1), 1.963(4); Mo(1)−N(3), 1.976(3); Mo(1)−S(2), 2.1677(12). Selected bond angles (deg): N(2)−Mo(1)−N(1), 115.9(2); N(2)−Mo(1)−N(3), 104.0(2); N(1)−Mo(1)−N(3), 110.97(14); N(2)−Mo(1)−S(2), 105.81(11); N(1)−Mo(1)−S(2), 103.62(10); N(3)−Mo(1)−S(2), 116.94(11).

distinct from one another in the solid state, it may be presumed that in solution at room temperature a fluxional process exchanges them rapidly since the solution ^2H NMR spectrum of the compound consists of a simple singlet.

The three complexes $Mo(E)(N[R]Ar)_3$ (E = S, Se, Te) were found in X-ray diffraction studies to exhibit pseudo mirror symmetry and to be essentially isostructural except for the Mo−E distance; see Figure 3−5 for ORTEP diagrams of $Mo(E)(N[R]Ar)_3$ (E = S, Se, Te). Selected distances and angles are given in the figure captions. The pseudo mirror symmetry in $Mo(S)(N[R]Ar)_3$ is such that the unique N(R)Ar ligand is that containing N(3).

The molybdenum−chalcogen distances were determined to be 2.1677(12), 2.3115(6), and 2.5353(6) Å, respectively, for E = S, Se, and Te. The Mo−S distance in $Mo(S)(N[R]Ar)_3$ is 0.09 Å shorter than those reported by Murphy and Parkin for *trans*-$S_2Mo(PR_3)_4$ complexes,[9] a result explicable on the basis

(13) Nugent, W. A.; Mayer, J. M. *Metal-Ligand Multiple Bonds*; Wiley: New York, 1988.

(14) Lappert, M. F.; Power, P. P.; Sanger, A. R.; Srivastava, R. C. *Metal and Metalloid Amides*; Ellis Horwood: Chichester, 1980.

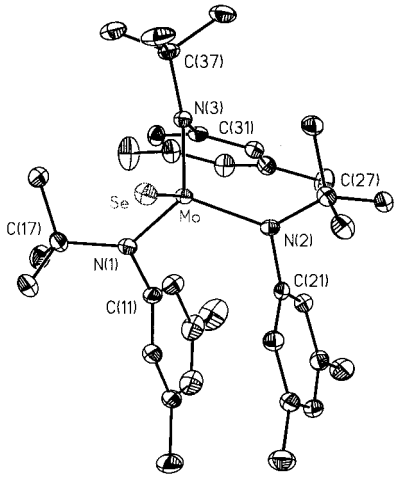

Figure 4. Structural drawing of $Mo(Se)(N[R]Ar)_3$ with thermal ellipsoids at the 35% probability level. Selected bond lengths (Å): Mo−N(1), 1.948(4); Mo−N(2), 1.967(4); Mo−N(3), 1.976(3); Mo−Se, 2.3115(6). Selected bond angles (deg): N(1)−Mo−N(2), 116.6(2); N(1)−Mo−N(3), 104.1(2); N(2)−Mo−N(3), 110.7(2); N(1)−Mo−Se, 105.49(11); N(2)−Mo−Se, 103.33(10); N(3)−Mo−Se, 117.03(10).

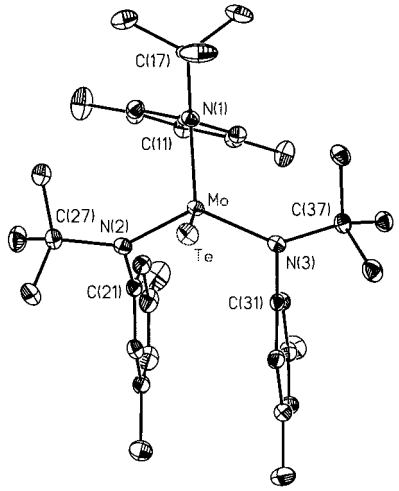

Figure 5. Structural drawing of $Mo(Te)(N[R]Ar)_3$ with thermal ellipsoids at the 35% probability level. Selected bond lengths (Å): Te−Mo, 2.5353(6); Mo−N(2), 1.938(2); Mo−N(3), 1.958(2); Mo−N(1), 1.978(2). Selected bond angles (deg): N(2)−Mo−N(3), 117.69(10); N(2)−Mo−N(1), 104.64(10); N(3)−Mo−N(1), 111.03(10); N(2)−Mo−Te 104.78(7); N(3)−Mo−Te, 102.37(7); N(1)−Mo−Te, 116.72(7).

of greater S−Mo π-bonding possible in $Mo(S)(N[R]Ar)_3$. The bis(sulfido) complexes *trans*-$S_2Mo(PR_3)_4$ can have at most an MoS double bond, while complex $Mo(S)(N[R]Ar)_3$ in principle can attain a MoS bond order of 2.5. By way of comparison with $Mo(Se)(N[R]Ar)_3$, the Mo−Se bond length in $[Mo(Se)_4]^{2-}$ is 2.293(1) Å.[15]

For each $Mo(E)(N[R]Ar)_3$ complex other than $Mo(O)(N[R]Ar)_3$, the two pseudo mirror related aryl rings engage in a parallel π-stacking arrangement, with *tert*-butyl groups oriented distal with respect to the center of the molecule. The third aryl group in each is essentially bisected by the pseudo mirror plane.

2.1.7. Electrochemistry. Cyclic voltammetry data for the four molybdenum(V) chalcogenide complexes $Mo(E)(N[R]Ar)_3$ are as follows ($E_{1/2}$): $Mo(O)(N[R]Ar)_3$, −0.92; $Mo(S)(N[R]Ar)_3$, −0.73; $Mo(Se)(N[R]Ar)_3$, −0.64; $Mo(Te)(N[R]Ar)_3$, −0.63. $E_{1/2}$ values for the electrochemically reversible oxidations were obtained in methylene chloride with saturated $[N(n\text{-}Bu)_4][PF_6]$ as the supporting electrolyte and are reported relative to the Cp_2Fe/Cp_2Fe^+ couple.[16]

The data indicate oxo $Mo(O)(N[R]Ar)_3$ to be the most reducing of the $Mo(E)(N[R]Ar)_3$ complexes, a result understandable if oxygen is, of the chalcogenides, best able to stabilize molybdenum's +6 oxidation state. From a synthetic point of view, the voltammetry data correlate with the observation that of the cations $[Mo(E)(N[R]Ar)_3]^+$ (E = O, S, Se, and Te), only $[Mo(O)(N[R]Ar)_3]^+$ proved to be isolable as iodide or triflate salts, as described below. Also consistent with the electrochemical data is the fact that the triflate salt of $[Mo(O)(N[R]Ar)_3]^+$ was not reduced to $Mo(O)(N[R]Ar)_3$ when mixed with solutions of the chalcogenide complexes $Mo(E)(N[R]Ar)_3$ (E = S, Se, and Te).

2.1.8. Thermochemistry. Solution calorimetry was used to obtain Mo−E bond dissociation enthalpies (BDEs) for $Mo(O)(N[R]Ar)_3$ and $Mo(S)(N[R]Ar)_3$. The heat of reaction of $Mo(N[R]Ar)_3$ with pyridine *N*-oxide (eq 3) was found to be -83.5 ± 1.4 kcal mol^{-1}. The bond dissociation enthalpy of pyridine *N*-oxide (*D*(NO), eq 4) has been determined to be 72.11 ± 0.67 kcal mol^{-1}.[17] Equation 5 represents the MoO bond dissociation enthalpy, *D*(MoO), for $Mo(O)(N[R]Ar)_3$ as 155.6 ± 1.6 kcal mol^{-1}, reflecting the assumption that ΔH_{rxn} (eq 5) = *D*(NO) − *D*(MoO).

$$Mo(N[R]Ar)_3 + ONC_5H_5 \rightarrow Mo(O)(N[R]Ar)_3 + NC_5H_5 \qquad \Delta H_{rxn} = -83.5 \pm 1.4 \text{ kcal mol}^{-1} \tag{3}$$

$$ONC_5H_5 \rightarrow [O] + NC_5H_5 \qquad \Delta H_{rxn} = 72.11 \pm 0.67 \text{ kcal·mol}^{-1} \tag{4}$$

$$Mo(O)(N[R]Ar)_3 \rightarrow [O] + Mo(N[R]Ar)_3 \qquad \Delta H_{rxn} = 155.6 \pm 1.6 \text{ kcal mol}^{-1} \tag{5}$$

Similarly, the heat of reaction of $Mo(N[R]Ar)_3$ with ethylene sulfide (eq 6) was experimentally determined to be -45.2 ± 1.2 kcal mol^{-1}. The energy required for dissociation of ethylene sulfide to give ethylene and atomic sulfur (eq 7) is 59.15 ± 0.33 kcal mol^{-1}, according to the literature.[18] Subtraction of eq 6 from eq 7 gives the molybdenum−sulfur bond dissociation enthalpy in $Mo(S)(N[R]Ar)_3$, accordingly taken (eq 8) to be 104.4 ± 1.2 kcal mol^{-1}.

$$Mo(N[R]Ar)_3 + SC_2H_4 \rightarrow Mo(S)(N[R]Ar)_3 + C_2H_4 \qquad \Delta H_{rxn} = -45.2 \pm 1.2 \text{ kcal mol}^{-1} \tag{6}$$

$$SC_2H_4 \rightarrow [S] + C_2H_4 \qquad \Delta H_{rxn} = 59.15 \pm 0.33 \text{ kcal mol}^{-1} \tag{7}$$

$$SMo(N[R]Ar)_3 \rightarrow [S] + Mo(N[R]Ar)_3 \qquad \Delta H_{rxn} = 104.4 \pm 1.2 \text{ kcal mol}^{-1} \tag{8}$$

The most critical assumption made in the foregoing analysis is that the measured heats of reaction correspond to differences in the indicated bond dissociation enthalpies. This seems a very reasonable approximation in the present case inasmuch as only

(15) O'Neal, S. C.; Kolis, J. W. *J. Am. Chem. Soc.* **1988**, *110*, 1971.
(16) Gritzner, G.; Kuta, J. *Pure Appl. Chem.* **1984**, *56*, 461.
(17) Shaofeng, L.; Pilcher, G. *J. Chem. Thermodyn.*, **1988**, *20*, 463.
(18) Cox, J. D.; Pilcher, G. *Thermochemistry of Organic and Organometallic Compounds*; Academic Press: New York, 1970. Chase, M. W. *JANAF Thermochemical Tables*; American Chemical Society: New York, 1986.

bonds to the chalcogen atom are made or broken. A small contribution to the enthalpy of reaction could conceivably arise from small changes in molybdenum−nitrogen bond lengths on going from molybdenum(III) to molybdenum(V); however, comparison of the structural data for $Mo(N[R]Ar)_3$ with those for $Mo(E)(N[R]Ar)_3$ (E = O, S) shows that the molybdenum−nitrogen distances are essentially the same for the three complexes despite the difference in formal oxidation state.

A second possible small contribution to the enthalpy of reactions in eqs 3 and 6 could stem from changes in preferred conformation of the three N(R)Ar ligands on going from $Mo(N[R]Ar)_3$ to $Mo(E)(N[R]Ar)_3$. The energetics of such structural changes were explored recently in a molecular mechanics study which indicated the presence of relatively small ($\leq\sim$6 kcal mol^{-1}) energy barriers separating the various possible conformations,[19] consistent with the fluxional nature of the compounds at 25 °C in solution on the ^{2}H and ^{1}H NMR time scales. Thus, the major contribution to the enthalpy of reaction is clearly ascribable to changes in Mo−E bonding accompanying the chalcogen atom transfer.

Heats of solvation for $Mo(N[R]Ar)_3$, $Mo(O)(N[R]Ar)_3$, and $Mo(S)(N[R]Ar)_3$ were measured and taken into account as detailed in the Experimental Section, or as detailed in the literature for the values pertaining to pyridine *N*-oxide and ethylene sulfide.

It should be noted that eqs 3 and 6 represent especially simple cases, since $Mo(N[R]Ar)_3$ is a neutral species possessing an empty coordination site, and the determinations of ΔH_{rxn} were made in toluene, a relatively nonpolar solvent. Only the bond of interest, that to the chalcogen, is broken and formed during the reaction.

In the context of oxo transfer chemistry, the strength of potential oxygen atom donors has been gauged by comparing bond dissociation enthalpies associated with (hypothetical) reactions of the type in eqs 4 and 5. Such numbers have been tabulated by Holm,[20] and their utility expounded on in the context of biologically relevant oxo transfer. It is of interest to note that $Mo(O)(N[R]Ar)_3$, with its D(MoO) of 155.6 ± 1.6 kcal mol^{-1}, possesses one of the strongest known transition metal−oxygen bonds.

Few data are available concerning metal−sulfur bond dissociation energies (as opposed to metal−oxygen); in this regard the data point obtained here for $Mo(S)(N[R]Ar)_3$ will serve as a useful reference.

A primary objective of the present study was to determine whether thermodynamic instability of $Mo(O)(N[R]Ar)_3$ renders eq 2 (deoxygenation of N_2O by $Mo(N[R]Ar)_3$) untenable. Obviously, the data presented in this section reveal $Mo(N[R]Ar)_3$ to be rather thermodynamically competent for deoxygenation of N_2O, the N−O BDE of which is known to be ca. 40 kcal mol^{-1}.[8] In fact, $Mo(N[R]Ar)_3$ possesses ca. 116 kcal mol^{-1} in excess of the deoxygenating power required for N_2O deoxygenation!

Two unknown quantities currently prevent quantitative enthalpic comparison of eqs 1 and 2, namely the nitrido Mo−N BDE for $Mo(N)(N[R]Ar)_3$ and the nitrosyl Mo−N BDE for $Mo(NO)(N[R]Ar)_3$. If we assume the former to be ca. 162 kcal mol^{-1},[21] then the latter would have to be only 75 kcal mol^{-1} for eqs 1 and 2 to be isothermic. Future studies may permit this comparison to be made on quantitative grounds.

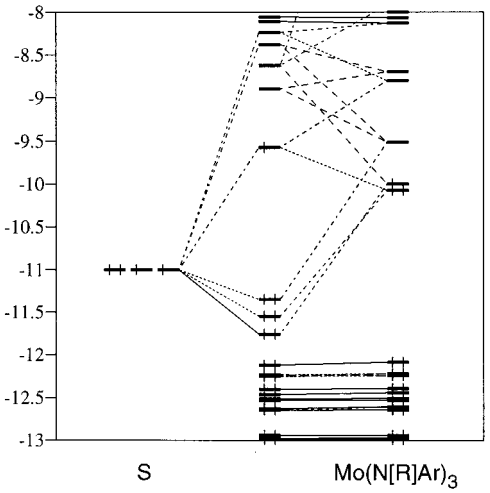

Figure 6. Representative fragment MO diagram showing the interaction of a chalcogen atom (S) with the pyramidal $Mo(N[R]Ar)_3$ fragment. From a whole-molecule calculation based on the X-ray structure of $Mo(S)(N[R]Ar)_3$.

Whatever the quantitative nature of the reaction enthalpy comparison between eqs 1 and 2, the origin of the selectivity in the reaction of $Mo(N[R]Ar)_3$ with N_2O also merits dissection in terms of kinetic parameters. Such a discussion is, however, outside of the scope of the present paper.

2.2. Theoretical Description of Mo(E)(N[R]Ar)$_3$ (E = O, S, Se, and Te). 2.2.1. Extended Hückel MO Analysis. Whole-molecule calculations were performed[22] using the X-ray crystal structure coordinates for the $Mo(E)(N[R]Ar)_3$ complexes. The goal was to understand qualitatively the Mo=E bonding and the nature of SOMO in the $Mo(E)(N[R]Ar)_3$ complexes. It was also of interest to compare these low-symmetry systems with C_3 analogues such as $Mo(N)(N[R]Ar)_3$. In the calculations, d-orbitals were not included for the chalcogen atoms and charge-iteration was not performed.

Inspection of Figure 6 shows that interaction of a sulfur atom with a pyramidal $Mo(N[R]Ar)_3$ fragment, in the geometry of $Mo(S)(N[R]Ar)_3$, leads to formation of three bonding and three antibonding interactions involving the sulfur 3p orbitals. Shown very clearly in the diagram is the fact that a large gap separates the SOMO from the next-highest-lying (SOMO-1) molecular orbital. This feature is illustrative of why the $Mo(E)(N[R]Ar)_3$ complexes undergo ready one-electron oxidations. A contour plot of the SOMO (not shown) indicates that this orbital is Mo−S π* in character. The SOMO-1 orbital was shown *via* a contour plot (not shown) to possess Mo−S π-bonding character. The diagram for $Mo(S)(N[R]Ar)_3$ is representative of those (not shown) calculated from the X-ray coordinates for the other $Mo(E)(N[R]Ar)_3$ complexes.

Other properties assessed *via* extended Hückel methodology were the molybdenum−chalcogenide overlap populations and net atomic charges. The overlap populations are as follows: Mo−O, 0.67; Mo−S, 1.10; Mo−Se, 0.81; Mo−Te, 0.74. By way of comparison, a similar calculation for $Mo(N)(N[R]Ar)_3$ gives an $Mo-N_{nitrido}$ overlap population of 1.11. These data indicate that, of the chalcogenides, sulfur is best matched in terms of orbital energetics and radial properties for interaction with molybdenum. The $Mo-N_{amido}$ overlap populations were found to be close to 0.60 for all of the compounds studied,

(19) Hahn, J.; Landis, C. R.; Nasluzov, V. A.; Neyman, K. M.; Rösch, N. *Inorg. Chem.* **1997**, *36*, 3947.

(20) Holm, R. H.; Donahue, J. P. *Polyhedron* **1993**, *12*, 571.

(21) Neyman, K. M.; Nasluzov, V. A.; Hahn, J.; Landis, C. R.; Rösch, N. *Organometallics* **1997**, *16*, 995.

(22) Landrum, G. A. YAeHMOP: Yet Another extended Molecular Orbital Package. YAeHMOP is freely available on the WWW at URL http://overlap.chem.cornell.edu:8080/yaehmop.html.

despite the geometric asymmetry of the $Mo(E)(N[R]Ar)_3$ complexes.

The fact that $Mo(O)(N[R]Ar)_3$ has a lower Mo−E overlap population than $Mo(S)(N[R]Ar)_3$ but a greater Mo−E bond strength is accounted for in terms of $Mo(E)(N[R]Ar)_3$ having a substantial ionic contribution to the bond strength. This is reflected in the net atomic charges as follows: Mo, O (+2.640, −1.417); Mo, S (+1.598, −0.322); Mo, Se (+2.417, −1.257); Mo, Te (+2.470, −1.348). By way of comparison, the net atomic charges for $Mo(N)(N[R]Ar)_3$ are: Mo, $N_{nitride}$ (+3.028, −1.863). Net charges for the N_{amido} nitrogens were close to −0.850 for all of the complexes studied. These results show clearly that, of the $Mo(E)(N[R]Ar)_3$ complexes, $Mo(O)(N[R]Ar)_3$ possesses the most ionic bond.

While the extended Hückel method is useful for illuminating bonding and energetic issues qualitatively, it is also of interest to compare the experimental data to results of density functional calculations on some simplified model complexes.

2.2.2. Density Functional Calculations. In order more quantitatively to elucidate the electronic and geometrical structures as well as thermodynamic parameters of the $Mo(E)(N[R]Ar)_3$ complexes, quantum chemical calculations of the model complexes $Mo(E)(NH_2)_3$ (E = O, S, Se, Te) were carried out. These calculations utilized the hybrid density functional B3LYP method[23] in conjunction with the double-ζ plus polarization quality basis set lanl2dz + d_E (α_d = 0.85, 0.503, 0.364 and 0.252 for O,[24] S, Se, and Te atoms,[25] respectively), which for heavy atoms (S, Se, Te, and Mo) uses the Hay and Wadt effective core potential (ECP) including relativistic effects for Mo and Te.[26] All calculations were performed using the GAUSSIAN-94 package.[27]

Gradient-corrected density functional methods such as B3LYP have been shown to be quite reliable in prediction of geometries and energies.[28] For instance, the B3LYP method describes the geometry of the model complex $(\mu\text{-}N_2)(Mo[(HNCH_2CH_2)_3N])_2$ very well in comparison with the experimental structure of the real system $(\mu\text{-}N_2)(Mo[(t\text{-}BuMe_2SiNCH_2CH_2)_3N])_2$, with the N−N distance of 1.22 Å (calculated) vs 1.20 Å (X-ray), the Mo−N(trans to N_2) distance of 2.30 Å (calculated) vs 2.29 Å (X-ray), and the other Mo−N distances of 1.97 Å (calculated) vs 2.01 Å (average, X-ray).[29]

As reported previously by Cui *et al.*,[28] the ground state of hypothetical $Mo(NH_2)_3$ is the quartet A′ state in C_{3h} symmetry with three unpaired electrons in the $d_{xz}(e'')$, $d_{yz}(e'')$, and $sd_{z^2}(a')$ orbitals. The doublet A′ state is calculated to be about 14.5 kcal mol^{-1} higher-lying. In C_3 symmetry, the addition of an O, S, Se, or Te atom in the ^3S state with two unpaired electrons to the quartet $Mo(NH_2)_3$ gives the doublet $Mo(E)(NH_2)_3$ complex with Mo−E bonding interactions consisting of one σ-component and a net 1.5 π-component. The relevant interaction diagram is qualitatively identical to the one calculated from extended Hückel methods shown in Figure 6.

2.2.3. DFT Structural Predictions. Geometry optimization on the model complexes $Mo(E)(NH_2)_3$ (E = S, Se, and Te) converges to a C_s conformation with a doublet A″ ground state. In contrast, $Mo(O)(NH_2)_3$ is calculated to have C_1 symmetry, albeit only slightly distorted from C_s, with a doublet A ground state. Pertinent Mo−E bond distances (Å) are as follows: Mo−O, 1.715; Mo−S, 2.162; Mo−Se, 2.302; Mo−Te, 2.506. The latter values compare quite well to those observed experimentally for the $Mo(E)(N[R]Ar)_3$ complexes (respectively 1.706(2), 2.1677(12), 2.3115(6), and 2.5353(6) Å). It may be noted that the particular C_s conformation calculated for the $Mo(E)(NH_2)_3$ (E = S, Se, and Te) complexes is a "two-up, one-down" conformation, whereas that observed experimentally for the $Mo(E)(N[R]Ar)_3$ complexes is a "one-up, two-down" conformation; the two conformations are only ca. 2 kcal mol^{-1} apart in energy according to the DFT predictions for the complexes. This discrepancy between theory and experiment is attributable to the steric effects of the bulky N(R)Ar ligands, in addition to intramolecular π-stacking effects, which together might be expected to overcome the small electronic energy difference between the two C_s conformations. The steric and/or intramolecular π-stacking effects also would be expected to result in bond angle discrepancies, and therefore, only bond distances and energies will be discussed further.

2.2.4. DFT Bond Energies. The $Mo(E)(NH_2)_3$ binding energies are calculated at the B3LYP/lanl2dz + d_E level to be 140.2, 94.1, 82.5, and 64.5 kcal mol^{-1} for E = O, S, Se, and Te, respectively. At this level of theory, the calculated values for $Mo(O)(NH_2)_3$ and $Mo(S)(NH_2)_3$ are 10% smaller than the experimentally determined ones (see above), 155.6 ± 1.6 and 104.3 ± 1.2 kcal mol^{-1}, respectively. The errors, in part due to the approximations used and in part due to the difference between the real and model systems, are expected to be systematic. Therefore, the $Mo(Se)(N[R]Ar)_3$ and $Mo(Te)(N[R]Ar)_3$ bond energies can be predicted to be 91 and 71 kcal mol^{-1}, respectively, by scaling up the calculated values for $Mo(Se)(NH_2)_3$ and $Mo(Te)(NH_2)_3$ by 10%.

2.2.5. DFT Population Analysis. The foregoing trends in the energies and geometries of the calculated complexes can be explained in terms of the electronegativity and the size of valence s and p orbitals of the O, S, Se, and Te atoms. The atomic electronegativity decreases in the order O > S ≈ Se > Te, and the radial extent of valence s and p orbitals increases in the same order. Therefore, one may expect that the electrostatic character of the Mo−E bond will decrease and its covalent character will increase in the order O, S ≈ Se, Te. From a DFT Mulliken population analysis, it may be seen that both the net positive charge on the metal center, +1.35, +1.16, +1.10, and +1.04, and the absolute value of the negative charge of the atom E, −0.46, −0.38, −0.32, and −0.29, decrease on going from O to Te; this confirms that the ionic character of the Mo−E bond actually decreases in the above order. At the same time, the overlap population between the Mo and E atoms, 0.68, 0.81, 0.86, and 0.87, increases in the same order, indicating that the covalent character of the Mo−E bond actually increases in this order.

(23) Becke, A. D. *Phys. Rev. A* **1988**, *38*, 3093. Becke, A. D. *J. Chem. Phys.* **1993**, *98*, 5648. Lee, C.; Yang, W.; Parr, R. G. *Phys. Rev. B* **1988**, *37*, 785.

(24) Dunning, J. T. H.; Hay, P. J. *Methods of Electronic Structure Theory*; Plenum Press: New York, 1977.

(25) Hollwarth, A.; Bohme, M.; Dapprich, S.; Ehlers, A. W.; Gobbi, A.; Jonas, V.; Kohler, K. F.; Stegmann, R.; Veldkamp, A.; Frenking, G. *Chem. Phys. Lett.* **1993**, *203*, 237.

(26) Hay, P. J.; Wadt, W. R. *J. Chem. Phys.* **1985**, *82*, 284. Hay, P. J.; Wadt, W. R. *J. Chem. Phys.* **1985**, *82*, 299.

(27) Frisch, M. J.; Trucks, G. W.; Schlegel, H. B.; Gill, P. M. W.; Johnson, B. G.; Robb, M. A.; Cheeseman, J. R.; Keith, T. A.; Petersson, G. A.; Montgomery, J. A.; Raghavachari, K.; Al-Laham, M. A.; Zakrzewski, V. G.; Ortiz, J. V.; Foresman, J. B.; Cioslowski, J.; Stefanov, B. B.; Nanayakkara, A.; Challacombe, M.; Peng, C. Y.; Ayala, P. Y.; Chen, W.; Wong, M. W.; Andres, J. L.; Replogle, E. S.; Gomperts, R.; Martin, R. L.; Fox, D. J.; Binkley, J. S.; DeFrees, D. J.; Baker, J.; Stewart, J.; Head-Gordon, M.; Gonzales, C.; Pople, J. A. *GAUSSIAN-94*; Gaussian Incorporated: Pittsburgh, PA, 1995.

(28) Cui, Q.; Musaev, D. G.; Svensson, M.; Sieber, S.; Morokuma, K. *J. Am. Chem. Soc.* **1995**, *117*, 12366. Ricca, A.; Bauschlicher, J. C. W. *J. Phys. Chem.* **1994**, *98*, 12899. Ricca, A.; Bauschlicher, J. C. W. *J. Phys. Chem.* **1995**, *99*, 5922.

(29) Shih, K.-Y.; Schrock, R. R.; Kempe, R. *J. Am. Chem. Soc.* **1994**, *116*, 8804.

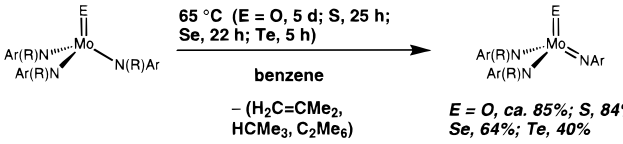

Figure 7. Synthetic protocol for the four Mo(E)(NAr)(N[R]Ar)$_2$ complexes.

A Mulliken spin density analysis suggests that the SOMO is localized more on the metal than on the E atom in the case of Mo(O)(NH$_2$)$_3$. The extent of localization decreases on going from O to Te. As E changes in this order, the lower electronegativity of E as well as the larger Mo(dπ)−E(pπ) overlap increases the contribution of E(pπ) to the π^* orbital, resulting in more delocalization and smaller spin density on molybdenum. These effects are reflected in the smoothly increasing separation (as a function of E) between g_1, g_2, and g_3 in the rhombic EPR spectra of the Mo(E)(N)[R]Ar)$_3$ complexes (see above).

2.3. Synthesis and Characterization of Mo(E)(NAr)(N[R]-Ar)$_2$ (E = O, S, Se, and Te). 2.3.1. Synthesis. Prolonged thermolysis of Mo(O)(N[R]Ar)$_3$ at temperatures of ∼65 °C resulted in conversion to a single new diamagnetic product, as assayed by ^{1}H and ^{2}H NMR spectroscopies (Figure 7). During the thermolysis, the color of the solution went from dark brown to a very light yellow-brown. In an experiment where the thermolysis was carried out in C_6D_6 and the volatiles subsequently examined by ^{1}H NMR spectroscopy, isobutylene, isobutane and hexamethylethane—the products of *tert*-butyl radical disproportionation and conproportionation—were observed.[30] A similar type of reaction involving *tert*-butyl radical elimination from a *tert*-butoxy molydenum(V) complex was reported recently.[31] Thermal conversion of d^1 oxo Mo(O)(N[R]-Ar)$_3$ to d^0 oxo imide Mo(O)(NAr)(N[R]Ar)$_2$ can be carried out conveniently on a scale of ca. 1 g. Unfortunately, Mo(O)(NAr)-(N[R]Ar)$_2$ proved to be an oily, difficult-to-purify species, samples of which often were contaminated with 5−10% of the amine H(N[R]Ar). Carrying out the thermolysis reaction at higher temperatures for shorter reaction times did not result in purer samples of Mo(O)(NAr)(N[R]Ar)$_2$.

Thermolysis of the molybdenum(V) sulfido complex Mo(S)-(N[R]Ar)$_3$ resulted in a color change from dark brown to a much lighter red-brown (Figure 7). The thermolysis also resulted in the formation of isobutylene, isobutane, and hexamethylethane (observed by ^{1}H and ^{2}H NMR) attributed to *tert*-butyl radical elimination, converting one of the N(R)Ar ligands into an imido (NAr) ligand with concomitant one-electron oxidation of the molybdenum center. Sulfide imide Mo(S)(NAr)(N[R]Ar)$_2$ was obtained as an orange powder in 84% yield subsequent to recrystallization (OEt$_2$, −35 °C).

Thermolysis of selenide Mo(Se)(N[R]Ar)$_3$ (65 °C, 22 h) gave a single molybdenum-containing product, with isobutane, isobutylene, and hexamethylethane appearing as byproducts (Figure 7). During the thermolysis, the reaction mixture's color changed from dark brown to a medium red-orange. Selenide imide Mo(Se)(NAr)(N[R]Ar)$_2$ is an orange-brown solid which was isolated in 64% yield subsequent to recrystallization (OEt$_2$, −35).

Thermolysis of telluride Mo(Te)(N[R]Ar)$_3$ produced one diamagnetic molybdenum-containing species assigned as Mo-(Te)(NAr)(N[R]Ar)$_2$ (Figure 7). Prolonged heating of mixtures containing Mo(Te)(NAr)(N[R]Ar)$_2$ gave rise to decomposition, possibly *via* a disproportionation reaction similar to that proposed for oxo Mo(O)(NAr)(N[R]Ar)$_2$. Substantial production of the free H(N[R]Ar) ligand also occurred, according to NMR spectroscopic monitoring. Thus, the optimal conditions for thermal conversion of Mo(Te)(N[R]Ar)$_3$ to Mo(Te)(NAr)-(N[R]Ar)$_2$ involved heating for no longer than ca. 5 h at 65 °C. These conditions provided ca. 80% conversion to Mo(Te)(NAr)-(N[R]Ar)$_2$, according to ^{2}H NMR monitoring. Recrystallization from ether gave Mo(Te)(NAr)(N[R]Ar)$_2$ as a dark brown powder (ca. 40% yield) which, despite repeated recrystallizations, failed to give satisfactory combustion analytical data.

2.3.2. NMR Data. ^{2}H NMR spectroscopy alone was not sufficient to distinguish between the following two possible isomers: (i) the oxo imide structure Mo(O)(NAr)(N[R]Ar)$_2$, and (ii) the aryloxide nitride formulation Mo(N)(OAr)(N[R]Ar)$_2$ derived from aryl group migration to the oxo function. Related rearrangements have recently been invoked to explain products of *tert*-butyl radical ejection from d^1 molybdenum *tert*-butoxide complexes.[31] Other characterization data (HRMS, ^{13}C NMR) also are consistent with either isomer.

It was possible to obtain ^{77}Se NMR data for Mo(Se)(NAr)-(N[R]Ar)$_2$, a single broad ($\Delta\nu_{1/2}$ = 46 Hz) resonance appearing at δ = 1923.4 ppm; coupling to ^{95}Mo/^{97}Mo was not observed. Although ^{77}Se NMR chemical shifts for metal selenido complexes are known to depend strongly on the attendant ligands, there are some general trends as follows. Terminal selenido complexes exhibit resonances appearing between 803 and 2397 ppm,[32] with the majority falling in the 1900−2300 ppm range.[33] By contrast, organoselenolate complexes have resonances typically falling between 200 and 1128 ppm.[34] The chemical shift observed for Mo(Se)(NAr)(N[R]Ar)$_2$ is therefore indicative of a terminal selenido functionality, as opposed to an organoselenolate function.

Telluride Mo(Te)(NAr)(N[R]Ar)$_2$ exhibits an extremely broad ^{125}Te NMR resonance at 2459.3 ppm ($\Delta\nu_{1/2}$ = 250 Hz); satellites indicative of coupling to ^{95}Mo/^{97}Mo were not observed. Terminal telluride complexes exhibit ^{125}Te signals ranging from 2700[35] to 3300 ppm, though some have been located at higher field.[9] Alkyl tellurides of tin[36] and iron[37] have chemical shifts of approximately −1200 ppm. Although relatively little data on ^{125}Te NMR shifts are extant in the literature, it has been suggested that a corrleation may exist for selenium and tellurium chemical shifts in related systems.[32] Thus, the chemical shift observed for Mo(Te)(NAr)(N[R]Ar)$_2$ seems indicative of the terminal telluride function as opposed to the alternative formulation, the aryl tellurolate.

2.3.3. Infrared Spectra. Possibly the most convincing evidence for formulation of the product of Mo(O)(N[R]Ar)$_3$ thermolysis as oxo imide Mo(O)(NAr)(N[R]Ar)$_2$ is an intense infrared stretch at 913 cm^{-1} ascribable to ν(MoO). This band is at higher energy than ν(MoO) for oxo complex Mo(O)(N[R]-Ar)$_3$ (893 cm^{-1}, *vide supra*), a change consistent with the

(30) Terry, J. O.; Futrell, J. H. *Can. J. Chem.* **1968**, 664. Weydert, M.; Brennan, J. G.; Andersen, R. A.; Bergman, R. G. *Organometallics* **1995**, *14*, 3942. Pryor, W. A. *Free Radicals*; McGraw-Hill: New York, 1966.
(31) Peters, J. C.; Johnson, A. R.; Odom, A. L.; Wanandi, P. W.; Davis, W. M.; Cummins, C. C. *J. Am. Chem. Soc.* **1996**, *118*, 10175.
(32) Rabinovich, D.; Parkin, G. *Inorg. Chem.* **1995**, *34*, 6341. Rabinovich, D.; Parkin, G. *Inorg. Chem.* **1994**, *33*, 2313.
(33) Ansari, M. A.; Ibers, J. A. *Coord. Chem. Rev.* **1990**, *100*, 223.
(34) Kraatz, H.-B.; Boorman, P. M.; Parvez, M. *Can. J. Chem.* **1993**, *71*, 1437. Fischer, H.; Zeuner, S.; Gerbing, U.; Riede, J.; Kreiter, C. J. *J. Organometal. Chem.* **1989**, *377*, 105. Ansari, M. A.; Mahler, C. H.; Ibers, J. A. *Inorg. Chem.* **1989**, *28*, 2669. Ball, J. M.; Boorman, P. M.; Fait, J. F.; Kraatz, H.-B.; Richardson, J. F.; Collison, D.; Mabbs, F. E. *Inorg. Chem.* **1990**, *29*, 3290.
(35) Shin, J. H.; Parkin, G. *Organometallics* **1994**, *13*, 2147.
(36) Seligson, A. L.; Arnold, J. *J. Am. Chem. Soc.* **1993**, *115*, 8214.
(37) Gindelberger, D. E.; Arnold, *J. Inorg. Chem.* **1993**, *32*, 5813.

expected increase in Mo−O bond order on going from a molybdenum(V) to a molybdenum(VI) terminal oxo moiety.

Complex Mo(S)(NAr)(N[R]Ar)$_2$ exhibits a strong infrared stretch at 506 cm^{-1}, a slightly higher energy ν(MoS) than that observed for the molybdenum(V) sulfide complex Mo(S)(N[R]-Ar)$_3$, supporting the proposed formulation of Mo(S)(NAr)(N[R]-Ar)$_2$ with terminal sulfido and imido ligands.

A strong far-IR peak at 355 cm^{-1} attributable to ν(MoSe) was observed for Mo(Se)(NAr)(N[R]Ar)$_2$, a value slightly higher in energy than that observed for molybdenum(V) selenido Mo(Se)(N[R]Ar)$_3$.

Complex Mo(Te)(NAr)(N[R]Ar)$_2$ exhibits a strong peak attributable to ν(MoTe) in the far-IR at 291 cm^{-1}, a value slightly higher in energy than that observed for the molybdenum(V) precursor Mo(Te)(N[R]Ar)$_3$. Literature values for metal-terminal telluride stretching frequencies are not prevalent; in the present case, the assignment was made by subtracting the spectrum of Mo(Te)(NAr)(N[R]Ar)$_2$ from that for selenide Mo(Se)(NAr)(N[R]Ar)$_2$.

2.3.4. Chemical Characterization of Mo(E)(NAr)(N[R]-Ar)$_2$. The product of Mo(O)(N[R]Ar)$_3$ thermolysis was hydrolyzed, and the resulting organic materials (according to a GCMS assay) included H(N[R]Ar) and H_2NAr, but not HOAr, consistent with the formulation Mo(O)(NAr)(N[R]Ar)$_2$.

In another attempt to differentiate between the two potential connectivities, Mo(O)(NAr)(N[R]Ar)$_2$ was allowed to react with benzaldehyde. Although the reaction proceeded only to the extent of ca. 10% under the conditions employed, both the imine Ph(H)C═NAr and the dioxo complex Mo(O)$_2$(N[R]Ar)$_2$ (see below) were observed spectroscopically, consistent with the oxo imido formuation; certain high-valent transition-metal imido complexes react with aldehydes to give imines, reactivity reminiscent of the phosphinimine-based imine synthesis (Wittig-type).[38]

Similarly, Mo(S)(NAr)(N[R]Ar)$_2$ was allowed to react with benzaldehyde. Spectroscopic evidence was consistent with gradual production of the imine Ph(H)C═NAr in small quantities, consistent with the presence of terminal imido and sulfido substituents in Mo(S)(NAr)(N[R]Ar)$_2$. Prolonged thermolysis of Mo(S)(NAr)(N[R]Ar)$_2$ gave decomposition to unknown products.

Prolonged thermolysis of Mo(O)(NAr)(N[R]Ar)$_2$ at elevated temperatures or storage of the oil at room temperature for extended periods appeared (^{1}H NMR) to give disproportionation to a mixture of Mo(O)$_2$(N[R]Ar)$_2$ and Mo(NAr)$_2$(N[R]Ar)$_2$. This reaction appears to result in an equilibrium mixture with $K_{eq} \approx 1$.

2.4. Kinetics of C−N Bond Homolysis for Mo(O)(N[R]-Ar)$_3$ and Mo(S)(N[R]Ar)$_3$. The kinetics of the thermolysis reaction of oxo Mo(O)(N[R]Ar)$_3$ was investigated by ^{2}H NMR spectroscopy in the temperature interval 65−105 °C. Disappearance of Mo(O)(N[R]Ar)$_3$ relative to an external concentric standard was monitored. The reaction was found to obey a first-order kinetic profile for several half-lives, the observed first-order rate constants ($\times 10^5$ s^{-1}) being 0.586 ± 0.067 (335.9 K), 1.86 ± 0.37 (345.7 K), 6.50 ± 2.09 (355.7 K), 22.8 ± 4.0 (365.8 K), and 67.4 ± 10.8 (377.0 K). Activation parameters derived from a fit of the data to the Eyring equation are as follows: $\Delta H^{\ddagger} = 28.85 \pm 0.05$ kcal mol^{-1}, $\Delta S^{\ddagger} = 3.10 \pm 0.08$ eu. These values are suggestive of substantial N−C bond breaking on going from ground to transition state and a transition state for N−C bond cleavage that is not particularly constrained. The data are consistent with a rate-determining step involving simple N−C bond homolysis.

The kinetic data for Mo(S)(N[R]Ar)$_3$ thermolysis are similar, except that the thermolysis is significantly more facile than for Mo(O)(N[R]Ar)$_3$, with first-order rate constants for Mo(S)(N[R]-Ar)$_3$ thermolysis ($\times 10^4$ s^{-1}) being 1.32 ± 0.27 (339.1 K), 2.25 ± 0.23 (343.3 K), 3.86 ± 0.62 (348.5 K), 8.94 ± 1.87 (355.9 K), and 20.1 ± 3.8 (366.0 K). Activation parameters derived from a fit of the data to the Eyring equation are as follows: $\Delta H^{\ddagger} = 24.39 \pm 0.13$ kcal mol^{-1}, $\Delta S^{\ddagger} = -4.53 \pm 0.06$ eu.

That the Mo(E)(N[R]Ar)$_3$ complexes are thermally unstable is easily understood in terms of the fragment MO diagram for Mo(S)(N[R]Ar)$_3$ given above (Figure 6), in which a large gap separates the SOMO from the next-highest-lying orbital. The odd electron in Mo(E)(N[R]Ar)$_3$ is effectively sloughed off as *tert*-butyl radical in the thermal conversion to the Mo(E)(NAr)-(N[R]Ar)$_2$ complexes.

2.5. Reactions of Mo(N[R]Ar)$_3$ with Various Chalcogen-Containing Compounds. 2.5.1. Reaction of Mo(N[R]Ar)$_3$ with NO$_2$. Mo(N[R]Ar)$_3$ is thermodynamically competent to reduce NO_2 with a reaction enthalpy of −82 kcal mol^{-1}. Ethereal Mo(N[R]Ar)$_3$ at 25 °C was treated with 0.5 equiv NO_2, eliciting a rapid color change to brown over 10 min. ^{1}H and ^{2}H NMR spectroscopic examination of the reaction mixture confirmed complete conversion of Mo(N[R]Ar)$_3$ to a mixture of Mo(O)(N[R]Ar)$_3$ and the known terminal nitrosyl complex Mo(NO)(N[R]Ar)$_3$.[1]

2.5.2. Reaction of Mo(N[R]Ar)$_3$ with SO$_2$. Mo(N[R]Ar)$_3$ is also thermodynamically competent to remove one oxygen from SO_2 with a reaction enthalpy of −24 kcal mol^{-1}. Treatment of ethereal Mo(N[R]Ar)$_3$ with 0.6 equiv of gaseous SO_2 resulted in an immediate color change to dark brown. Analysis of the reaction mixture confirmed the presence of oxo Mo(O)(N[R]Ar)$_3$ and sulfide Mo(S)(N[R]Ar)$_3$ in a 2:1 ratio as determined by ^{2}H NMR spectroscopy. Mo(N[R]Ar)$_3$ had been completely consumed. This reaction represents a rare example of clean activation of SO_2 to give sulfido and oxo ligands where the fate of all of the reactants and the product distribution are known.[39] Oxidation of the crude reaction mixture with iodine showed conversion to the oxo iodide [Mo(O)(N[R]Ar)$_3$][I] and the same decomposition products observed subsequent to iodine oxidation of Mo(S)(N[R]Ar)$_3$.

2.5.3. Reaction of Mo(N[R]Ar)$_3$ with OSMe$_2$. Mo(N[R]-Ar)$_3$ is thermodynamically capable of deoxygenating $OSMe_2$ (see above). Accordingly, treatment of Mo(N[R]Ar)$_3$ with $OSMe_2$ led to formation of a dark brown product in ca. 10 min. ^{2}H NMR analysis showed greater than 90% conversion of Mo(N[R]Ar)$_3$ to the oxo complex Mo(O)(N[R]Ar)$_3$.

2.5.4. Reaction of Mo(N[R]Ar)$_3$ with CS$_2$. Addition of 1 equiv of CS_2 to ethereal Mo(N[R]Ar)$_3$ led to rapid darkening of the mixture to a green-brown color. Analysis by ^{2}H NMR at this point indicated complete conversion of Mo(N[R]Ar)$_3$ to two products, namely, paramagnetic Mo(S)(N[R]Ar)$_3$ and diamagnetic (μ-CS)[Mo(N[R]Ar)$_3$]$_2$ in a 1:1 ratio (Figure 8). Separation of (μ-CS)[Mo(N[R]Ar)$_3$]$_2$ and Mo(S)(N[R]Ar)$_3$ proved difficult; the best analytical data for (μ-CS)[Mo(N[R]-Ar)$_3$]$_2$ are presented in the Experimental Section. Activation of CS_2 by transition metals is the subject of a somewhat dated review,[40] but this report does not describe the formation of

(38) Wigley, D. E. *Prog. Inorg. Chem.* **1994**, *42*, 239.

(39) Kubas, G. J. *Acc. Chem. Res.* **1994**, *27*, 183. Ellis, R.; Henderson, R. A.; Hills, A.; Hughes, D. L. *J. Organomet. Chem.* **1987**, *333*, C6. Lorenz, I.-P.; Walter, G.; Hiller, W. *Chem. Ber.* **1990**, *123*, 979.

(40) Butler, I. S.; Fenster, A. E. *J. Organomet. Chem.* **1974**, *66*, 161.

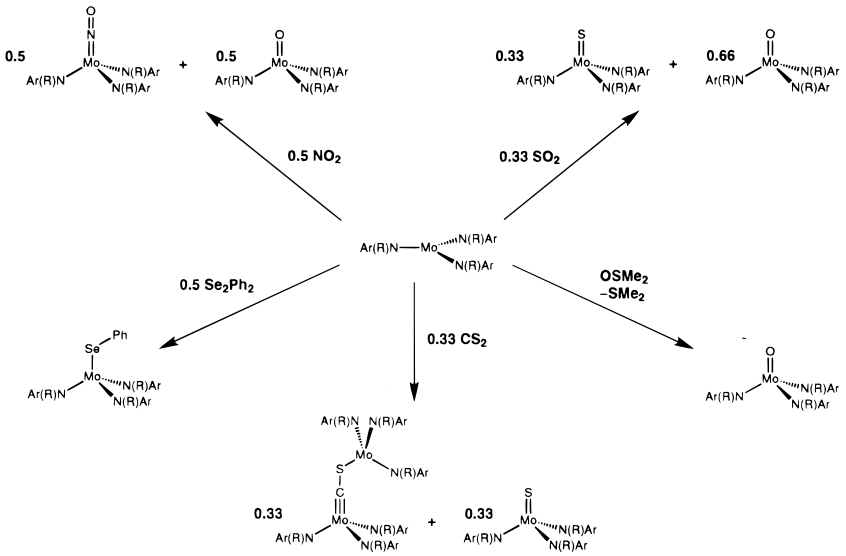

Figure 8. Various reactions of $Mo(N[R]Ar)_3$ with chalcogen-containing compounds. The reactions were carried out by addition of the reagent to a vessel containing ethereal $Mo(N[R]Ar)_3$.

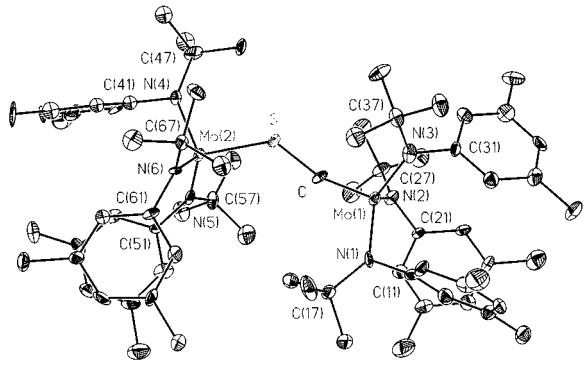

Figure 9. Structural drawing of $(\mu\text{-Cs})[Mo(N[R]Ar)_3]_2$ with thermal ellipsoids at the 35% probability level. Selected bond lengths (Å): Mo(1)−C, 1.751(12); Mo(1)−N(1), 1.968(10); Mo(1)−N(2), 1.990(10); Mo(1)−N(3), 1.999(11); Mo(2)−N(5), 1.959(11); Mo(2)−N(6), 1.960(10); Mo(2)−N(4), 1.990(10); Mo(2)−S, 2.289(3). Selected bond angles (deg): C−S−Mo(2), 130.5(5); S−C−Mo(1), 162.7(8); C−Mo(1)−N(1), 104.5(5); C−Mo(1)−N(2), 104.3(5); C−Mo(1)−N(3), 102.9(5); N(5)−Mo(2)−S, 110.2(3); N(6)−Mo(2)−S, 106.8(3); N(4)−Mo(2)−S, 102.3(3).

bridging thiocarbonyl complexes, though some are known.[41] Thiocarbonyl $(\mu\text{-CS})[Mo(N[R]Ar)_3]_2$ was examined by IR spectroscopy, but no distinct band corresponding to ν(CS) was identified. The stretching frequency for this functional group is expected to be in the range of 1150−1230 cm^{-1}.[41] ^1H NMR spectroscopy showed two distinct ligand environments, corresponding to the inequivalent ends of the molecule. The thiocarbonyl carbon is strongly deshielded, appearing at 293.5 ppm in the ^{13}C NMR spectrum of $(\mu\text{-CS})[Mo(N[R]Ar)_3]_2$.

2.5.5. X-ray Structure of $(\mu\text{-CS})[Mo(N[R]Ar)_3]_2$. Thiocarbonyl $(\mu\text{-CS})[Mo(N[R]Ar)_3]_2$ was studied by single-crystal X-ray diffraction. Because of some disorder in the molecule, as well as two disordered diethyl ether molecules in the asymmetric unit, the structure is of marginal quality; however, it reveals clearly the atom connectivity and gross geometrical features (Figure 9). The μ-CS linkage is bent at sulfur, with a C−S−Mo(2) angle of 130.5(5)°. In this respect, the MoS bond is presumed to be analogous to a thiolate linkage, with the sulfur acting as a four-electron $1\sigma,1\pi$ donor to the molybdenum. The Mo(1)−C−S angle of 162.7° is more bent than one expects for an alkylidyne, but the deviation from linearity is understandable in terms of the voluminous nature of the angular −SMo(N[R]-Ar)$_3$ substituent. The Mo−C bond distance of 1.751(12) Å and the Mo−S bond distance of 2.289(3) Å are similar to those reported for $(\eta^6\text{-}C_6H_5Me)(CO)_2Cr(\mu\text{-CS})Cr(CO)_5$, where the Cr−C bond distance is 1.747(5) Å and the Cr−S distance is 2.486(2) Å. The latter chromium complex is the only other structurally characterized μ_2,η^2-bridging thiocarbonyl complex found in a search of the Cambridge Structural Database (Lotz, ref 41). Another related bridging thiocarbonyl complex is (*tert*-$Bu_3SiO)_3Ta(\mu\text{-CS})Ta(SiO\text{-}t\text{-}Bu_3)$.[42]

The bond lengths in $(\mu\text{-CS})[Mo(N[R]Ar)_3]_2$ are indicative of MoC triple bonding, CS single bonding, and SMo $\sigma + \pi$ bonding. Thus, the formal oxidation states are molybdenum(VI) for the carbon-bound Mo atom and molybdenum(IV) for the sulfur-ligated Mo center. The molecule is intriguing in that it exhibits the two most common arrangements for an array of three −N(R)Ar ligands in a single molecule. The alkylidyne-like component is pseudo C_3 symmetric, while the thiolate-like end displays pseudo C_s symmetry. The CMoNC dihedral angles are 18.0, 23.0, and 32.5°, while on the other end of the molecule the SMoNC dihedral angles are 1.0, 38.8, and 50.8°. This type of arrangement seems to be general. Molecules such as $Mo(N)(N[R]Ar)_3$,[2] $Mo(NO)(N[R]Ar)_3$,[1] $Mo(P)(N[R]Ar)_3$,[4] and $Ti(Cl)(N[R]Ar)_3$,[43] are not subject to a Jahn−Teller distortion and display pseudo C_3 symmetric three-bladed propellor arrangements of the −N(R)Ar ligands. Meanwhile, molecules having an odd number of electrons in the Mo−apical-ligand π-system or molecules possessing single-electron-pair π-donors (e.g., thiolate, selenolate, or amide) in conjunction with a d^n (n = 1 or 2) electron count exhibit pseudo C_s symmetry.

2.5.6. Reaction of $Mo(N[R]Ar)_3$ with Se_2Ph_2. Addition of 0.5 equiv of Se_2Ph_2 to a solution of $Mo(N[R]Ar)_3$ in ether resulted in the formation of a brilliant blue-green diamagnetic complex, $Mo(SePh)(N[R]Ar)_3$, which was isolated in 72% yield (Figure 8). Phenyl selenide $Mo(SePh)(N[R]Ar)_3$ exhibits a ^{77}Se NMR chemical shift of 1006.3 ppm, with an extremely broad $\Delta\nu_{1/2}$ of 600 Hz. This chemical shift falls in the region typical

(41) Dombek, B. D.; Angelici, R. J. *Inorg. Chem.* **1976**, *15*, 2397. Kolb, O.; Werner, H. *Angew. Chem.* **1982**, *94*, 207. Lotz, S.; Pille, R. R.; Van Rooyen, P. H. *Inorg. Chem.* **1986**, *25*, 3053.

(42) Neithamer, D. R. Ph.D. Dissertation, Cornell University, 1989.

(43) Johnson, A. R.; Wanandi, P. W.; Cummins, C. C.; Davis, W. M. *Organometallics* **1994**, *13*, 2907.

of organoselenolate complexes,[34] though it is at the low-field edge of the usual range. The diamagnetism of the molecule is suggestive of an acute Mo−Se−C angle, reminiscent of the angular Mo−S−C function observed for (μ-CS)[Mo(N[R]Ar)$_3$]$_2$ (see above).

2.6. Compounds not Readily Deoxygenated by Mo(N[R]-Ar)$_3$. Several conceivable reactions of Mo(N[R]Ar)$_3$ which appear to be thermodynamically viable have turned out to be kinetically nonviable. There is no observable reaction of Mo(N[R]Ar)$_3$ with CO_2 (either 1 equiv, 10 equiv, or 1 atm) in a sealed reaction vessel at 25 °C, even though this reaction should be thermodynamically downhill by almost 30 kcal mol^{-1}. Although we have not performed a detailed theoretical analysis of the (hypothetical) reaction of Mo(N[R]Ar)$_3$ with CO_2, the observed lack of reaction is gratifyingly reminiscent of the selectivity of Mo(N[R]Ar)$_3$ for reaction with the NN versus the NO bond of nitrous oxide; CO_2 and N_2O are isoelectronic and both possess exceedingly large HOMO−LUMO gaps.

Deoxygenation of MeNCO by Mo(N[R]Ar)$_3$ is estimated to be thermodynamically favorable by 46 kcal mol^{-1}, in view of the known bond dissociation enthalpies. Treatment of Mo(N[R]-Ar)$_3$ with excess *t*-BuNCO (neat) gave a very small (≤5%) extent of conversion to oxo Mo(O)(N[R]Ar)$_3$ and Mo(CN-*t*-Bu)(N[R]Ar)$_3$ over 24 h at 25 °C. The latter species was detected by ^{2}H NMR spectroscopy and is presumably analogous to known Mo(CO)(N[R]Ar)$_3$.[44]

The reaction of Mo(N[R]Ar)$_3$ with $OPPh_3$ is estimated to be downhill by 22 kcal mol^{-1}, but as was the case for CO_2, no reaction was observed. In the case of $OPPh_3$, it may be that the combined steric bulk of the two reactants prevents oxo transfer. In a control experiment, oxo Mo(O)(N[R]Ar)$_3$ was allowed to react with PPh_3 with the result, again, that no reaction was observed. Evidently, large activation barriers inhibit transfer of an oxo moiety between Mo(N[R]Ar)$_3$ and PPh_3, in both directions.

The enthalpy of reaction of Mo(N[R]Ar)$_3$ with O_2SMe_2 is calculated to be favorable by 43 kcal mol^{-1}. This reaction is intriguing in that the second deoxygenation of the oxidant is more favorable at 68 kcal mol^{-1}. Therefore, for each molecule of O_2SMe_2 which reacts, 2 equiv of Mo(O)(N[R]Ar)$_3$ would be expected to form. However, over a 48 h period, there was essentially no conversion of Mo(N[R]Ar)$_3$ to Mo(O)(N[R]Ar)$_3$ (1 equiv of O_2SMe_2, THF, 25 °C).

2.7. Reactions of Mo(O)(N[R]Ar)$_3$ with Oxidants. 2.7.1. Reaction with One-Electron Oxidants. Oxo Mo(O)(N[R]Ar)$_3$ is oxidized to an oxomolybdenum(VI) cation upon treatment with either ferrocenium triflate[45] or iodine, generating the corresponding triflate [Mo(O)(N[R]Ar)$_3$][O_3SCF_3] or iodide [Mo(O)(N[R]Ar)$_3$][I] salts (Figure 10). Addition of [Cp_2Fe]-[O_3SCF_3] to an ethereal solution of Mo(O)(N[R]Ar)$_3$ resulted in gradual precipitation of an orange-brown solid over 15 h. The triflate salt [Mo(O)(N[R]Ar)$_3$][O_3SCF_3] was subsequently isolated in 71% yield. The IR spectrum of [Mo(O)(N[R]Ar)$_3$]-[O_3SCF_3] evinces a strong peak at 972 cm^{-1} attributable to ν(MoO) and peaks indicative of an ionic rather than a covalently bound triflate.[46] Addition of 0.5 equiv of I_2 to ethereal Mo(O)(N[R]Ar)$_3$ resulted in rapid precipitation of [Mo(O)(N[R]-Ar)$_3$][I] as an orange solid, which was isolated in 88% yield. Salt [Mo(O)(N[R]Ar)$_3$][I] exhibited a strong band in its IR spectrum at 975 cm^{-1}, attributable to ν(MoO). The iodide and triflate salts of [Mo(O)(N[R]Ar)$_3$]$^+$ tended to decompose slightly during attempted recrystallization (THF, CH_2Cl_2), the iodide salt being especially sensitive; this sensitivity precluded analysis by ^{13}C NMR. Combustion analytical data for the iodide and triflate salts of [Mo(O)(N[R]Ar)$_3$]$^+$ also are poor, presumably due to thermal decomposition of the samples.

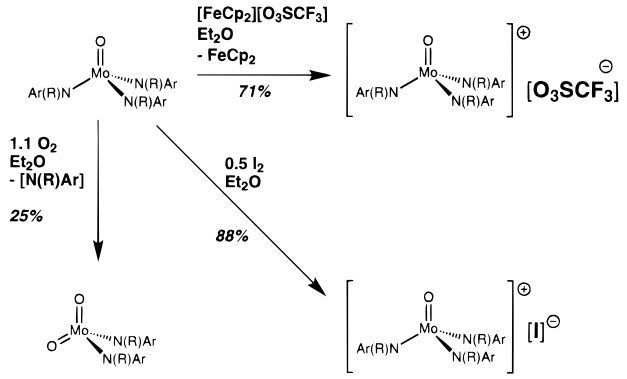

Figure 10. Reactions of Mo(O)(N[R]Ar)$_3$ with oxidizing agents.

Related oxidations of Mo(E)(N[R]Ar)$_3$ (E = S, Se, and Te) attempted in an effort to generate analogs of [Mo(O)(N[R]Ar)$_3$]-[I] and [Mo(O)(N[R]Ar)$_3$][O_3SCF_3] were unrewarding. The putative salt [Mo(S)(N[R]Ar)$_3$][O_3SCF_3] was detected spectroscopically but could not be isolated. Rapid catastrophic decomposition occurred upon addition of ferrocenium triflate or elemental iodine to Mo(Te)(N[R]Ar)$_3$. Presumably, the desired salt forms and decomposes rapidly to unknown products.

2.7.2. Reaction with Dioxygen. Treatment of Mo(O)-(N[R]Ar)$_3$ with 1.1 equiv of dry O_2 gave a gradual color change from dark brown to a much darker brown (Figure 10). After approximately 12 h, the reaction mixture had attained a deep red-brown color. Analysis of the reaction mixture by ^{1}H NMR revealed formation of H(N[R]Ar) and Mo(O)$_2$(N[R]Ar)$_2$ in approximately a 2:1 ratio. Dioxo Mo(O)$_2$(N[R]Ar)$_2$ was recovered from the mixture in low yield as bright yellow crystals. The complex exhibits two strong ν(MoO) peaks in the IR at 943 and 920 cm^{-1}, corresponding well to literature data for related dioxo species.[47]

The use of an excess of dioxygen in the synthesis of Mo(O)$_2$-(N[R]Ar)$_2$ was found to be essential. Treatment of Mo(O)-(N[R]Ar)$_3$ with 0.5 equiv of O_2 over a similar time period gave only 50% consumption of Mo(O)(N[R]Ar)$_3$ according to ^{2}H NMR spectroscopic analysis.

Small amounts of dioxo Mo(O)$_2$(N[R]Ar)$_2$ were sometimes detected spectroscopically among the myriad of products resulting from reactions of Mo(N[R]Ar)$_3$ with dioxygen in various stoichiometries and under various conditions. Under no conditions tested could either monoxo Mo(O)(N[R]Ar)$_3$ or dioxo Mo(O)$_2$(N[R]Ar)$_2$ be obtained in useful synthetic quantities from the direct reaction of Mo(N[R]Ar)$_3$ with dioxygen. This nonresult contrasts starkly with chemistry observed for Cr(N[R]Ar$_F$)$_3$, which is known to react with O_2 (excess) to provide the chromium analog of Mo(O)$_2$(N[R]Ar)$_2$, Cr(O)$_2$(N[R]-Ar$_F$)$_2$, in high yield.[48] In addition, Chisholm and co-workers have shown that the molybdenum(III) dimer Mo$_2$(O-*t*-Bu)$_6$ reacts smoothly with dioxygen giving dioxo O_2Mo(O-*t*-Bu)$_2$ in good yield, a reaction presumed to occur via expulsion of *tert*-butoxy radical.[47]

(44) Peters, J. C.; Odom, A. L.; Cummins, C. C. *Chem. Commun.* **1997**, 1995.
(45) Schrock, R. R.; Sturgeoff, L. G.; Sharp, P. R. *Inorg. Chem.* **1983**, *22*, 2801.
(46) Lawrance, G. A. *Chem. Rev.* **1986**, *86*, 17.
(47) Chisholm, M. H.; Folting, K.; Huffman, J. C.; Kirkpatrick, C. C. *Inorg. Chem.* **1984**, *23*, 1021.
(48) Odom, A. L.; Cummins, C. C. Manuscript in preparation.

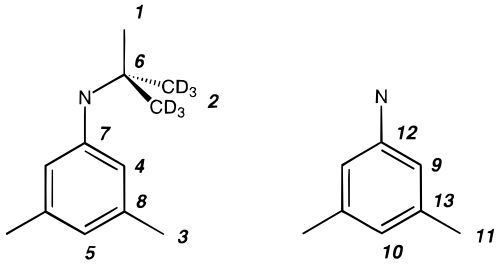

Figure 11. Numbering scheme for NMR assignments. At left is shown the intact amido ligand, and on the right is depicted the imido ligand resulting from *tert*-butyl elimination.

3. Concluding Remarks

This paper describes experimental and theoretical work inspired by the observation that $Mo(N[R]Ar)_3$ reacts selectively with nitrous oxide giving N−N bond cleavage products as opposed to oxo abstraction. Theoretical and experimental observations indicate that the Mo═O bond is quite strong and that, therefore, an instability of this linkage cannot be used to rationalize the observed selectivity in the nitrous oxide reaction (eq 1).

In the course of the work, a series of molybdenum(V) chalcogenide complexes, $Mo(E)(N[R]Ar)_3$, E = O, S, Se, and Te, were isolated and characterized. It was also discovered that the latter complexes undergo upon thermolysis a C−N bond homolysis reaction, giving rise to *tert*-butyl radical elimination and formation of the arylimidomolybdenum(VI) functional group.

Reactions of chalcogen atom donors with $Mo(N[R]Ar)_3$ were surveyed. The results were intriguing in that certain potential oxo donors (e.g., CO_2, $OPPh_3$, and OCN-*t*-Bu) failed to react with $Mo(N[R]Ar)_3$ despite moderately favorable thermodynamics. More potent chalcogenido donors (e.g., NO_2, SO_2, $OSMe_2$, ONC_5H_5, and CS_2) did, on the other hand, react readily with $Mo(N[R]Ar)_3$ to give terminal chalcogenide complexes.

This research should be viewed in the context of the remarkable selectivity of the reaction of $Mo(N[R]Ar)_3$ with nitrous oxide (eq 1).[1] Ongoing research is aimed at elucidating a more complete mechanistic picture of this singular small-molecule-activation reaction.

4. Experimental Section

4.1. General Considerations. General experimental details are as reported previously[49] except as noted otherwise. OEt_2 was dried according to a procedure by Grubbs.[50] Other solvents were distilled under nitrogen from sodium benzophenone ketyl. Toluene used for EPR spectroscopy was vacuum transferred from *tert*-butyllithium. $Mo(N[R]Ar)_3$ was prepared according to the literature procedure.[2] Other chemicals were purified and dried by standard procedures or were used as received. Solution magnetic susceptibilities were measured by the NMR technique.[51] ^1H and ^{13}C NMR spectra were recorded on Varian XL-300, Varian Unity-300, or Brucker AC-250 spectrometers. Chemical shift assignments are reported with reference to Figure 11 and are relative to internal solvent (7.15 and 128.0 ppm, respectively for ^1H and ^{13}C NMR spectra recorded in C_6D_6). ^2H NMR chemical shifts are reported with respect to external C_6D_6 (7.15 ppm). ^{77}Se NMR spectra were recorded on a Varian Unity-300 or a Varian XL-500 spectrometer and are referenced to Me_2Se (0 ppm) by comparison to external Se_2Ph_2 ($CDCl_3$ 460 ppm). ^{125}Te NMR spectra were recorded on a Varian XL-500 spectrometer and referenced to Me_2Te (0 ppm) by comparison to external $TeCl_4$ (HCl/H_2O, 1237 ppm). EPR spectra were recorded on a Brucker ESP-300 spectrometer. EPR samples in toluene were sealed in quartz tubes, and spectra were recorded either at ambient temperature or at low temperature using a liquid-nitrogen-cooled nitrogen stream. Spectra were simulated using the program EPR-NMR;[52] EPR spectra for the $Mo(E)(N[R]Ar)_3$ complexes have already appeared in print.[53] Infrared measurements were carried out on a Bio-Rad FTS-135 spectrometer. Far-IR measurements were carried out on a Mattson Instruments IR-10110 spectrometer. Electrochemical measurements were carried out at room temperature (28 °C) in a glovebox with ~1×10^{-3} M CH_2Cl_2 solutions containing saturated $[N(n\text{-}Bu)_4][PF_6]$ as the supporting electrolyte. The standard three electrode system consisted of platinum working and counter electrodes with a silver reference electrode. Platinum electrodes were pretreated by polishing with diamond paste. Potentials are referenced to the ferrocene/ferrocenium couple.[54] C, H, and N microanalyses were performed by Oneida Research Services (Whitesboro, NY) or Microlytics (South Deerfield, MA). Melting points were obtained in sealed glass capillaries and are uncorrected.

4.2. SQUID Magnetic Measurements. Data were acquired as reported previously using a Quantum Design SQUID magnetometer.[49] The magnetometer uses the MPMSR2 software (Magnetic Property Measurement System Revision 2). Data were recorded from 5 to 300 K at a field strength of 5000 G. The raw SQUID data and fits for the $Mo(E)(N[R]Ar)_3$ complexes have already appeared in print.[53]

4.3. Kinetics Measurements. A sample of $Mo(O)(N[R]Ar)_3$ or $Mo(S)(N[R]Ar)_3$ (ca. 0.02 M in benzene) was placed in an NMR tube along with a sealed capillary filled with a D_2O/THF solution (1:20 by weight). The tube was flame sealed and stored at 4 °C. Constant temperature oil baths were employed for the thermolysis reaction. NMR tubes were placed in the oil bath for a measured time interval and then immediately placed in an ice-water slush. Loss of starting material was assessed by intergration of peaks in the ^2H NMR spectrum. The signal for $Mo(O)(N[R]Ar)_3$ was integrated from 9.2 to 5.2 ppm, the peak for $Mo(S)(N[R]Ar)_3$ was integrated from 7.8 to 4.8 ppm, and the D_2O peak was integrated from 3.6 to 4.6 ppm (relative to external C_6H_6). The tubes were then replaced in the oil bath for another time interval. The heating/measurement cycles were repeated for 3−4 half-lives. The measured first-order rate constants *k* are reported with their respective 95% confidence intervals. Activation parameters were obtained from the relation of the derived first-order rate constants with temperature using the Eyring equation. Raw kinetic data for thermolyses of $Mo(E)(N[R]Ar)_3$ (E = O, S) have already appeared in print.[53]

4.4. Synthesis of $Mo(O)(N[R]Ar)_3$. ONC_5H_5 (0.1014 g, 0.9467 mmol) was added to a solution of $Mo(N[R]Ar)_3$ (0.5844 g, 0.9090 mmol) in OEt_2 (15 mL). The slurry was stirred for 3.5 h, at which time all of the ONC_5H_5 had dissolved and the solution had turned dark brown. The solvent was removed, the product was extracted with fresh OEt_2, and the extract was filtered. Crystallization from OEt_2 gave dark brown faceted crystals (0.4311 g, 0.6543 mmol, 72%): mp 134−135 °C (dec.). ^2H NMR (46 MHz, toluene): $\delta = 7.62$ ($\Delta\nu_{1/2} = 30$ Hz). ^1H NMR (300 MHz, C_6H_6): $\delta = 7.2$ (br s, 1), 0.0895 (br s, 3). IR (benzene/KBr, 2 cm^{-1}): ν(MoO) = 891 cm^{-1}. UV/vis (ether): λ_{max} (nm) = 212 (ϵ 53 000). EPR (toluene, 25 °C): $g = 1.96$, $a(^{95}Mo/^{97}Mo) = 35.7$ G. EPR (toluene, 101 K): $g_1 = 1.990$, $g_2 = 1.967$, $g_3 = 1.937$. MS (70 eV) *m*/*z* (%): 654.5 (3.8) [M^+]. μ_{eff} (300 MHz, C_6D_6, 22.6 °C): 2.19 μ_B. SQUID (5-300 K): $\mu_{eff} = 1.664$ μ_B. CV (CH_2Cl_2/$[N(n\text{-}Bu)_4][PF_6]$): $E_{1/2} = -0.92$ V. Anal. Calcd for $C_{36}H_{39}D_{15}MoN_3O$: C, 65.93; H, 8.30; N, 6.41. Found: C, 66.22; H, 8.50; N, 6.19.

4.5. Synthesis of $Mo(S)(N[R]Ar)_3$. A solution of $Mo(N[R]Ar)_3$ (0.4303 g, 0.6693 mmol) in OEt_2 (6 mL) was added to a slurry of S_8 (0.0322 g, 0.1255 mmol, 1.5 eq) in OEt_2 (5 mL) eliciting a rapid color change to purple and then brown after about 5 min. The reaction

(49) Johnson, A. R.; Davis, W. M.; Cummins, C. C. *Organometallics* **1996**, *15*, 3825.
(50) Pangborn, A. B.; Giardello, M. A.; Grubbs, R. H.; Rosen, R. K.; Timmers, F. J. *Organometallics* **1996**, *15*, 1518.
(51) Sur, S. K. *J. Magn. Reson.* **1989**, *82*, 169.
(52) Mombourquette, M. J.; Weil, J. A.; McGavin, D. G. *Computer Program EPR-NMR*; University of Saskatchewan, Canada: Department of Chemistry, 1993.
(53) Johnson, A. R. Ph.D. Dissertation, Massachusetts Institute of Technology, 1997.
(54) Bard, A. J.; Faulkner, L. R. *Electrochemical Methods*; John Wiley & Sons: New York, 1980.

mixture was stirred overnight, subsequent to which the OEt_2 was removed in vacuo. The residue was extracted with pentane, the extract was filtered, and the crude material thereby obtained was recrystallized from OEt_2 (3 mL) at −35 °C (0.2865 g, 0.4245 mmol, 63%): mp 110−112 °C (dec). ^{2}H NMR (46 MHz, OEt_2): $\delta = 6.545$ ($\Delta\nu_{1/2} = 22.0$ Hz). ^{1}H NMR (300 MHz, C_6D_6): $\delta = \approx 6.0$ (br s, 1), −1.1 (br s, 3). IR (benzene/KBr): ν(MoS) = 491 cm^{-1}. EPR (toluene, 25 °C): $g = 1.96$, $a(^{95}Mo/^{97}Mo) = 28.5$ G. EPR (toluene, 107 K): $g_1 = 1.996$, $g_2 = 1.970$, $g_3 = 1.922$, $a_3(^{95}Mo/^{97}Mo) = 54$ G. MS (70 eV) *m*/*z* (%): 671 (0.22) [M$^+$]. $\mu_{eff} = 1.630\ \mu_B$. CV (CH_2Cl_2/[N(*n*-Bu)$_4$][PF_6]): $E_{1/2} = -0.73$ V. Anal. Calcd for $C_{36}H_{42}D_{12}MoN_3S$: C, 64.64; H, 8.14; N, 6.28. Found: C, 64.94; H, 8.31; N, 6.23.

4.6. Synthesis of Mo(Se)(N[R]Ar)$_3$. Solid Mo(N[R]Ar)$_3$ (0.5008 g, 0.7790 mmol) and Se (0.0810 g, 0.790 mmol) were added to a vessel containing OEt_2 (10 mL), and the resulting mixture was stirred for 11 h. The solution was filtered to remove excess Se, and the filtrate was concentrated. Three crops of crystals were collected subsequent to recrystallization from OEt_2 at −35 °C (0.4519 g, 0.6260 mmol, 80.4%): mp 128−130 °C. ^{1}H NMR (300 MHz, C_6D_6): $\delta \approx 6.5$ (br s, 1), −1.412 (br s, 3). ^{2}H NMR (46 MHz, OEt_2): $\delta = 7.036$ ($\Delta\nu_{1/2} = 30.7$ Hz). IR (benzene/polyethylene): ν(MoSe) = 342 cm^{-1}. EPR (toluene, 25 °C): $g = 1.97$, $a(^{95}Mo/^{97}Mo) = 30.5$ G. EPR (toluene, 98 K): $g_1 = 2.030$, $a_1(^{95}Mo/^{97}Mo) = 29$ G, $g_2 = 1.986$, $g_3 = 1.899$, $a_3(^{95}Mo/^{97}Mo) = 48$ G. UV/vis (ether): $\lambda_{max} = 403$ nm (ϵ 6270); 487 nm (ϵ 2410). MS (70 eV) *m*/*z* (%): 658.2 (18.11) [M$^+$ − C(CD$_3$)$_2$-CH$_3$]. SQUID (5−300 K): 1.75 μ_B. CV (CH_2Cl_2/[N(*n*-Bu)$_4$][PF_6]): $E_{1/2} = -0.64$ V. Anal. Calcd for $C_{36}H_{36}D_{18}MoN_3Se$: C, 59.90; H, 7.54; N, 5.82. Found: C, 60.25; H, 7.41; N, 5.68.

4.7. Reaction of Mo(N[R]Ar)$_3$ with PEt$_3$. Solid Mo(N[R]Ar)$_3$ (0.0503 g, 0.0782 mmol) was dissolved in OEt_2 (2 mL), and PEt_3 (15 μL, 0.102 mmol, 1.3 eq) was added. The reaction mixture was stirred for 18 h and then examined by ^{2}H NMR. The spectrum revealed only the presence of unreacted Mo(N[R]Ar)$_3$.

4.8. Synthesis of Mo(Te)(N[R]Ar)$_3$. Solid Mo(N[R]Ar)$_3$ (0.5035 g, 0.7832 mmol) and Te (0.1188 g, 0.9310 mmol) were added to a vessel containing OEt_2 (10 mL) leading to an orange solution. PEt_3 (20 μL, 0.14 mmol, 0.17 equiv) was then added, and the reaction mixture was stirred for 18 h, during which time the mixture acquired a dark brown color. The OEt_2 was removed in vacuo, the resulting residue was extracted with THF, and the extract was filtered and concentrated. Recrystallization from OEt_2 (ca. 25 mL) at −35 °C produced spectroscopically pure Mo(Te)(N[R]Ar)$_3$ (2 crops, 0.4422 g, 0.5739 mmol, 73%): mp 127−128 °C (dec.). ^{2}H NMR (46 MHz, ether): $\delta = 8.120$ ($\Delta\nu_{1/2} = 22.9$ Hz). ^{1}H NMR (300 MHz, ether): $\delta = 8.120$ ($\Delta\nu_{1/2} = 22.9$ Hz). ^{1}H NMR (300 MHz, C_6D_6): $\delta \approx 8$ (br S, 1), −1.9 (br s, 3). IR (benzene/polyethylene): ν(MoTe) = 286 cm^{-1}. EPR (toluene, 25 °C): $g = 1.977$. EPR (toluene, 105 K): $g_1 = 2.130$, $a_1(^{95}Mo/^{97}Mo) = 28$ G, $g_2 = 1.970$, $a_2(^{95}Mo/^{97}Mo) = 24$ G, $g_3 = 1.850$, $a_3(^{95}Mo/^{97}Mo) = 48$ G. UV/vis (ether): $\lambda_{max} = 486$ nm (ϵ = 6314). MS (70 eV) *m*/*z* (%): 707.3 (38.24) [M$^+$ − C(CD$_3$)$_2$CH$_3$]. SQUID (5−180 K): 1.86 μ_B. CV (CH_2Cl_2/[N(*n*-Bu)$_4$][PF_6]): $E_{1/2} = -0.63$ V. Anal. Calcd for $C_{36}H_{42}D_{12}MoN_3Te$: C, 56.12; H, 7.06; N, 5.45. Found: C, 56.50; H, 7.33; N, 5.17.

4.9. Synthesis of Mo(O)(NAr)(N[R]Ar)$_2$. A solution of Mo(O)-(N[R]Ar)$_3$ (0.4422 g, 0.6879 mmol) in C_6H_6 (10 mL) was heated (65 °C) until the dark brown color, characteristic of Mo(O)(N[R]Ar)$_3$, faded to a much lighter yellow (ca. 5 d). Solvent was removed in vacuo, yielding, essentially quantitatively by weight, a yellow oil. ^{1}H NMR spectroscopy indicated the oil to consist of Mo(O)(NAr)(N[R]Ar)$_2$ (approximately 85% pure, contaminated with HN(R)Ar). ^{1}H NMR (300 MHz, C_6D_6): $\delta = 6.912$ (s, 4); 6.885 (s, 5); 6.712 (s, 9); 6.52 (s, 10); 2.139 (s, 3); 2.026 (s, 11); 1.340 (s, 1). ^{13}C NMR (75 MHz, $CDCl_3$): $\delta = 6.912$ (s, 4); 6.885 (s, 5); 6.712 (s, 9); 6.52 (s, 10); 2.139 (s, 3); 2.026 (s, 11); 1.340 (s, 1). ^{13}C NMR (75 MHz, $CDCl_3$): $\delta = 156.365$ (s, 12); 150.510 (s, 7); 137.712 (s, 13); 137.560 (s, 8); 128.304 (d, 4); 127.373 (d, 9); 120.702 (d, 10); 120.008 (d, 5); 60.555 (s, 6); 31.496 (q, 1); 30.090 (m, 2); 21.237 (q, 3); 21.143 (q, 11). IR (benzene/KBr): ν(MoO) = 913 cm^{-1}. MS (70 eV) *m*/*z* (%): 594.3 (1.77) [M$^+$]. HRMS (70 eV): calcd mass (597.336989); found (597.33709).

4.10. Synthesis of Mo(S)(NAr)(N[R]Ar)$_2$. Mo(S)(N[R]Ar)$_3$ (0.1640 g, 0.2430 mmol) was dissolved in benzene (10 mL) and heated at 62.5 °C in a sealed bomb for 25 h. The solution changed from dark brown to red-brown. The benzene was removed in vacuo, and an orange powder was obtained from OEt_2 (0.1250 g, 0.2043 mmol, 84.1%): mp 183−4 °C. ^{1}H NMR (300 MHz, C_6D_6): $\delta = 7.204$ (s, 5); 7.15 (s, 4); 6.710 (s, 9); 6.587 (s, 10); 2.145 (s, 3); 2.041 (s, 6H, 11); 1.310 (s, 6H, 1). ^{13}C NMR (75 MHz, $CDCl_3$): $\delta = 157.545$ (s, 12); 151.53 (s, 7); 138.27 (s, 13); 137.87 (s, 8); 129.77 (d, 4 or 9); 128.60 (br d, 4 or 9); 127.711 (d, 5 or 10); 119.87 (d, 5 or 10); 62.385 (s, 6); 31.957 (q, 1); 31.447 (m, 2); 21.481 (q, 3 and 11). IR (benzene/KBr): ν(MoS) = 506 cm^{-1}. MS (70 eV) *m*/*z* (%): 613 (44.1) [M$^+$]. Anal. Calcd for $C_{32}H_{33}D_{12}MoN_3S$: C, 62.82; H, 7.41; N, 6.87. Found: C, 63.11; H, 7.56; N, 6.76.

4.11. Synthesis of Mo(Se)(NAr)(N[R]Ar)$_2$. Mo(Se)(N[R]Ar)$_3$ (0.6377 g, 0.8834 mmol) and C_6H_6 (30 mL) were loaded into a sealable glass bomb and evacuated to autogenic pressure. The mixture was heated at 65 °C for 22 h at which point the solution had changed from the dark brown initial color to red-orange. The benzene was removed *in vacuo*, and the product was precipitated from OEt_2 (∼15 mL) as a finely divided orange brown powder in 2 crops (0.3733 g, 0.5667 mmol, 64%): mp 201.5−202 °C. ^{1}H NMR (300 MHz, C_6D_6): $\delta = 7.304$ (s, 9); 7.15 (s, 4); 6.713 (s, 5); 6.601 (s, 10); 2.145 (s, 3); 2.052 (s, 11); 1.290 (s, 1). ^{13}C NMR (75 MHz, $CDCl_3$): $\delta = 157.243$ (s, 12); 150.940 (s, 7); 138.027 (q, 13); 137.613 (q, 8); 129.454 (d); 128.612 (br m, 4); 127.438 (d); 119.225 (d); 62.20 (s, 6); 31.517 (q, 1); 31.0 (m, 2); 21.101 (q, 3 and 11). ^{77}Se NMR (57.292 MHz, $CDCl_3$, pw = 15 ms, d1 = 1 s, 16000 scans): $\delta = 1923.4$ ($\Delta\nu_{1/2} = 46.2$ Hz) relative to Me_2Se. IR (benzene/polyethylene): ν(MoSe) = 355 cm^{-1}. UV/vis (ether): λ_{max} = 292 nm (ϵ 17700). MS (70 eV) *m*/*z* (%): 660 (5) [M$^+$]. Anal. Calcd for $C_{32}H_{33}D_{12}MoN_3Se$: C, 58.35; H, 6.89; N, 6.38. Found: C, 58.79; H, 6.94; N, 6.24.

4.12. Synthesis of Mo(Te)(NAr)(N[R]Ar)$_2$. Mo(Te)(N[R]Ar)$_3$ (0.5085 g, 0.6600 mmol) was dissolved in C_6H_6 (25 mL) and evacuated to autogenic pressure. The solution was heated at 65 °C for 5 h; no color change was observed. The C_6H_6 was removed in vacuo leaving a fine dark red-brown powder (0.3712 g, 0.5248 mmol, 80%) which was contaminated with about 5% HN(R)Ar. The complex can be recrystallized from OEt_2 in low yield (∼40%): mp 194.5−195.5 °C. ^{1}H NMR (300 MHz, $CDCl_3$): $\delta = 7.3$ (br s, 4); 7.032 (s, 5 or 9); 6.916 (s, 10); 6.886 (s, 5 or 9); 6.4 (br s, 4); 2.350 (s, 11); 2.278 (s, 3); 1.131 (s, 1). ^{13}C NMR (75 MHz, $CDCl_3$): $\delta = 157.624$ (s, 12); 149.799 (s, 7); 138.412 (q, 13); 137.947 (q, 8); 131.2 (br d, 4); 129.548 (d); 127.776 (d); 127.0 (br d, 4); 119.116 (d); 62.6735 (s, 6); 31.4322 (q, 1); 30.9061 (m, 2); 21.2830 (q, 3); 21.2226 (q, 11). ^{125}Te NMR (158 MHz, $CDCl_3$, pw = 12 ms, d1 = 1 s, 28000 scans): δ: 2459.3 ($\Delta\nu_{1/2}$ = 250 Hz). IR (benzene/polyethylene): ν(MoTe) = 291 cm^{-1}. UV/vis (OEt_2): λ_{max} = 327 nm (ϵ 13 700). MS (70 eV) *m*/*z* (%): 705.2 (70) [M$^+$]. Anal. Calcd for $C_{32}H_{33}D_{12}MoN_3Te$: C, 54.34; H, 6.41; N, 5.94. Found: C, 51.30; H, 6.42; N, 5.39.

4.13. Synthesis of [Mo(O)(N[R]Ar)$_3$][O_3SCF_3]. Mo(O)(N[R]Ar)$_3$ (0.0996 g, 0.1512 mmol) in OEt_2 was added to a slurry of [Cp_2Fe]-[O_3SCF_3] (0.0512 g, 0.1528 mmol) in OEt_2 to a total volume of 5 mL. The solution was stirred for 15 h, at which point the solution was brown and an orange brown precipitate was observed. The solid (0.0865 g, 0.1071 mmol, 71%) was collected on a frit and washed with ether; the washings were colorless: mp 100−101 °C (dec.). ^{1}H NMR (300 MHz, $CDCl_3$): $\delta = 7.094$ (s, 5); 5.5 (br s, 4); 2.221 (br s, 3); 1.428 (br s, 1). ^{19}F NMR (282 MHz, $CDCl_3$): $\delta = -83.417$. ^{13}C NMR (125 MHz, $CDCl_3$): 148.083, 139.397, 131.501, 125.394 (4), 70.547 (6), 31.227 (1), 30.739 (2), 21.564 (3). IR (Nujol/KBr): 1601.8, 1266.1 (ionic triflate),[46] 1221.8, 1146.4, 1111.1, 1031.1 (ionic triflate),[46] 971.8 (ν-MoO), 698.8, 637.3, 570.7, 474.0 cm^{-1}. Anal. Calcd for $C_{37}H_{36}D_{18}F_3MoN_3O_4S$: C, 55.00; H, 6.74; N, 5.20. Found: C, 56.67; H, 6.94; N, 4.89.

4.14. Synthesis of [Mo(O)(N[R]Ar)$_3$][I]. To a solution of Mo(O)-(N[R]Ar)$_3$ (0.0999 g, 0.1516 mmol) in OEt_2 was added iodine (0.0199 g, 0.0784 mmol, 0.52 equiv) in OEt_2 giving a total volume of 5 mL. An orange precipitate formed rapidly. The solution was stirred for 15 h, at which point the supernatant was colorless. The orange solid (0.1042 g, 0.1326 mmol, 87.5%) was collected on a frit and washed with ether; the washings were colorless. The complex decomposed fairly rapidly in solvents in which it was soluble, precluding charac-

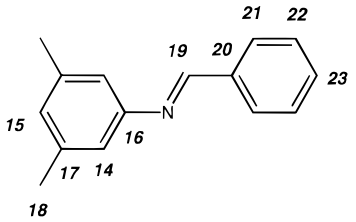

Figure 12. Numbering scheme for NMR assignments for the imine Ph(H)C═NAr.

terization by ^{13}C NMR and purification by recrystallization. The reported analysis is of isolated and washed material: mp 95−97 °C (dec.). ^{1}H (300 MHz, $CDCl_3$): $\delta = 7.079$ (s, 5); 5 (br s, 4); 2.214 (br s, 3); 1.428 (br s, 1). IR (Nujol/KBr, cm^{-1}): 1602.1, 1582.8, 1285.0, 1147.6, 1110.8, 1051.3, 1030.6, 974.5 (ν(MoO)), 939.1, 886.3, 701.1, 696.2. Anal. Calcd for $C_{36}H_{36}D_{18}IMoN_3O$: C, 55.03; H, 6.93; N, 5.35. Found: C, 54.17; H, 6.99; N, 5.14.

4.15. Generation of Ph(H)C═NAr for Spectroscopic Identification. Benzaldehyde (8.12 g, 76.5 mmol) and 3,5-dimethylaniline (10.23 g, 84.43 mmol) were mixed in C_6H_6 (30 mL) and heated to reflux for 6 h. Water was collected with a Dean−Stark trap (1.2 mL, 0.87 equiv) yielding a thick yellow oil (16.22 g) which was 95% pure by ^{1}H NMR. NMR assignments are with reference to the numbering scheme in Figure 12. ^{1}H NMR (300 MHz, C_6H_6): $\delta = 8.284$ (s, 19); 7.923 (m, 21); 7.196 (m, 22 and 23); 6.946 (s, 14); 6.786 (s, 15); 2.223 (s, 18). ^{13}C NMR (75 MHz, $CDCl_3$): $\delta = 159.934$ (d, 15); 152.176 (d, 16 or 20); 138.795 (q, 17); 136.446 (s, 16 or 20); 131.288 (dt, 23); 128.800 (d, 22); 127.729 (d, 21 or 14); 118.753 (d, 21 or 14); 113.204 (d, 19); 21.3884 (q, 18). MS (70 eV) *m*/*z* (%): 209.2 (100) [M$^+$]. HRMS (70 eV): calcd mass (209.120450); found (209.12038).

4.16. Synthesis of Mo(O)$_2$(N[R]Ar)$_2$. Mo(O)(N[R]Ar)$_3$ (0.2198 g, 0.3336 mmol) was dissolved in OEt_2 (15 mL) in a reaction bomb. Dioxygen (45.96 mL, 150 Torr, 0.371 mmol, 1.11 equiv) was added. After 80 min, the reaction mixture was dark brown. After 14 h, the reaction mixture was rich dark red-brown. An aliquot was examined by ^{1}H NMR, showing the presence of Mo(O)$_2$(N[R]Ar)$_2$ and H(N[R]-Ar) in a 1:2 ratio as the major products. Examination of the reaction mixture by ^{2}H NMR indicated consumption of all paramagnetic material. The solvent was removed in vacuo, and the resulting oily solid was dissolved in a minimum of hexane (ca. 2 mL). A dark brown solid was collected, which could be recrystallized from hexane yielding a dark yellow solid (0.0410 g, 0.0832 mmol, 25%): mp 129−130 °C. ^{1}H NMR (300 MHz, C_6H_6): $\delta = 6.761$ (s, 5); 6.666 (s, 4); 2.074 (s, 3); 1.227 (s, 1). ^{13}C NMR (125 MHz, $CDCl_3$): $\delta = 148.390$ (s, 7); 138.369 (s, 8); 128.855 (d, 5); 127.602 (d, 4); 61.54 (s, 6); 30.976 (q, 1); 30.611 (m, 2); 21.476 (q, 3). IR (KBr/C_6H_6): ν(MoO) = 943, 920 cm^{-1}. MS (70 eV) *m*/*z* (%): 491.8 (17.6) [M$^+$]. Anal. Calcd for $C_{24}H_{24}D_{12}MoN_2O_2$: C, 58.52; H, 7.37; N, 5.69. Found: C, 58.74; H, 7.36; N, 5.64.

4.17. Synthesis of (μ-CS)[Mo(N[R]Ar)$_3$]$_2$. CS_2 (50 mL, 0.5187 mmol, 0.66 equiv) was added to a solution of Mo(N[R]Ar)$_3$ (0.5034 g, 0.7831 mmol) in OEt_2 (25 mL). The solution rapidly turned dark greenish brown. ^{2}H NMR at this point showed a 1:1 mixture of the terminal sulfide complex and the bridging thiocarbonyl complex. Solvent was removed in vacuo leaving a foamy solid which was dissolved in OEt_2 (∼3 mL). Upon standing for about 30 s, a dark solid began to precipitate. More OEt_2 was added to fully dissolve the solid (∼10 mL), and the solution was stored at −35 °C. The first crop of solid was diamagnetic but additional crops were contaminated with Mo(S)(N[R]Ar)$_3$ (as measured by ^{2}H NMR) (0.1640 g, 0.1233 mmol, 47%): mp 139−140 °C. ^{1}H NMR (300 MHz, $CDCl_3$); $\delta =$ 6.711 (s, 5); 6.5681 (s, 5); 6.455 (br s, 4); 5.718 (s, 4); 2.199 (s, 3); 2.112 (s, 3); 1.285 (br s, 1). ^{13}C NMR (125 MHz, $CDCl_3$): $\delta = 293.51$ (br s, CS); 153.42 (br s, 7); 151.10 (s, 7), 136.20 (m, 8); 136.00 (m, 8); 131.02 (d); 127.67 (d); 126.96 (d); 126.39 (d); 63.57 (br s, 6); 61.30 (s, 6); 33.69 (q, 1); 33.01 (m, 2); 31.99 (q, 1); 31.33 (m, 2); 21.69 (q, 3); 21.60 (q, 3). UV/vis (ether): $\lambda_{max} = 363$ nm (ϵ 27 300); 438 nm (ϵ 9660); 582 nm (ϵ 3090). Anal. Calcd for $C_{73}H_{72}D_{36}Mo_2N_6S$: C, 65.93; H, 8.19; N, 6.32. Found: C, 64.74; H, 8.18; N, 6.18.

4.18. Synthesis of Mo(SePh)(N[R]Ar)$_3$. Se_2Ph_2 (0.1273 g, 0.4078 mmol, 0.52 equiv) was dissolved in OEt_2 (10 mL) and added to a solution of Mo(N[R]Ar)$_3$ (0.5063 g, 0.7876 mmol) in OEt_2 (20 mL). The solution rapidly changed to dark green-blue. The solvent was removed in vacuo, and the resulting blue-green solid was recrystallized from OEt_2 (0.4520 g, 0.5657 mmol, 71.8%): mp 141−142 °C. See Figure 12 for the phenyl group numbering scheme. ^{1}H NMR (300 MHz, $CDCl_3$): $\delta = 8.09$ (d, 21); 7.38 (t, 22); 7.29 (t, 23); 6.48 (s, 5); 6.05 (br s, 4); 2.10 (s, 3); 1.25 (s, 1). ^{13}C NMR (75 MHz, $CDCl_3$): $\delta =$ 152.03 (s, 7); 148.5 (s, 20); 136.04 (s, 4); 133.72 (d); 128.33 (d); 127.57 (br d); 126.62 (d); 125.35 (d); 62.67 (s, 6); 31.11 (q, 1); 30.62 (m, 2); 21.652 (q, 3). ^{77}Se NMR (95.4 MHz, $CDCl_3$, pw = 8 ms, d1 = 1 s, 14 400 scans): $\delta = 1006.3$ ($\Delta\nu_{1/2} \approx 600$ Hz). UV/vis (ether): l (nm) = 255 (ϵ 5000); 421 (ϵ 5970); 582 (ϵ 2490). Anal. Calcd for $C_{42}H_{41}D_{18}MoN_3Se$: C, 63.14; H, 7.44; N, 5.26. Found: C, 63.38; H, 7.67; N, 5.28.

4.19. Reaction of Mo(N[R]Ar)$_3$ with SO$_2$. Mo(N[R]Ar)$_3$ (0.0219 g, 0.0341 mmol) was dissolved in OEt_2 (5 mL) in an evacuated reaction bomb. SO_2 (0.50 mL, 0.020 mmol, 0.58 equiv) was added via syringe, causing a rapid color change to dark brown. Examination of the reaction mixture by ^{2}H NMR showed the presence of the Mo(O)(N[R]-Ar)$_3$ ($\delta = 7.41$) and the sulfido complex ($\delta = 6.46$ ppm) in approximately a 2:1 ratio. The peaks were not base line resolved, preventing an accurate integral to be obtained.

4.20. Reaction of Mo(N[R]Ar)$_3$ with NO$_2$. Mo(N[R]Ar)$_3$ (0.0203 g, 0.0316 mmol) was dissolved in OEt_2 (5 mL) in an evacuated reaction bomb. NO_2 (0.42 mL, 0.017 mmol, 0.54 equiv) was added via syringe, causing a color change to pale tan-brown over 10 min. Examination of the reaction mixture by ^{2}H NMR showed the presence of the oxo complex ($\delta = 7.57$) and diamagnetic material ($\delta = 2.16$) in a ratio of 1:1. The solvent was removed in vacuo, and the reaction mixture was examined by ^{1}H NMR, clearly showing that the only diamagnetic product was Mo(NO)(N[R[Ar)$_3$.

4.21. Reaction of Mo(N[R]Ar)$_3$ with OSMe$_2$. Mo(N[R]Ar)$_3$ (0.0201 g, 0.0313 mmol) was dissolved in OEt_2 (3 mL) and $OSMe_2$ (2.5 mL, 0.0352 mmol, 1.1 equiv) was added. After 10 min, the reaction mixture was dark brown. Examination of the reaction mixture by ^{2}H NMR showed Mo(N[R]Ar)$_3$ ($\delta = 63.95$) and Mo(O)(N[R]Ar)$_3$ ($\delta = 7.59$) in a 1:9 ratio.

4.22. Reaction of Mo(N[R]Ar)$_3$ with OPPh$_3$. Mo(N[R]Ar)$_3$ (0.0400 g, 0.0622 mmol) and $OPPh_3$ (0.0260 g, 0.0934 mmol, 1.5 equiv) were dissolved in toluene (5 mL) under an atmosphere of Ar and stored at −35 °C for 24 h. The solution was then warmed to room temperature. Analysis of the reaction mixture by ^{2}H NMR showed the presence of Mo(N[R]Ar)$_3$ ($\delta = 62.99$), Mo(O)(N[R]Ar)$_3$ ($\delta = 7.1$), and diamagnetic material ($\delta = 1.53$) in a 5:2:1 ratio. Analysis of the reaction mixture by ^{31}P NMR showed the presence of $OPPh_3$ ($\delta =$ 25.00). The reaction was stirred at room temperature for 24 h, at which point ^{2}H NMR analysis revealed the presence of Mo(N[R]Ar)$_3$ ($\delta =$ 63.27), an unknown paramagnetic material ($\delta = 23.46$), Mo(O)(N[R]-Ar)$_3$ ($\delta = 7.22$), and diamagnetic material ($\delta = 1.49$) in a 3:1:1:1 ratio. ^{31}P NMR analysis again only showed the presence of $OPPh_3$ ($\delta =$ 25.00). Analysis of the reaction mixture by ^{1}H NMR showed primarially H(N[R]Ar).

4.23. Reaction of Mo(N[R]Ar)$_3$ with CO$_2$. Mo(N[R]Ar)$_3$ (0.0500 g, 0.0778 mmol) was dissolved in OEt_2 (ca. 5 mL) in a reaction bomb, and CO_2 (ca. 25 mL, 1 atm, 1.0 mmol, 13 equiv) was added. After 1 h at 0 °C, the reaction mixture was examined by ^{2}H NMR, showing Mo(N[R]Ar)$_3$ ($\delta = 64$) and Mo(O)(N[R]Ar)$_3$ ($\delta = 7.5$) in a 18:1 ratio. The reaction was repeated and allowed to react at 0 °C for 24 h. Examination of the reaction mixture by ^{2}H NMR showed Mo(N[R]-Ar)$_3$ ($\delta = 63.6$), Mo(CO)(N[R]Ar)$_3$ ($\delta = 10.0$),[44] Mo(O)(N[R]Ar)$_3$ and other material ($\delta = 7-8$), and diamagnetic material ($\delta = 2.13$) in approximately a 20:1:10:20 ratio.

4.24. Reaction of Mo(N[R]Ar)$_3$ with *t*-BuNC. Mo(N[R]Ar)$_3$ (0.0204 g, 0.0317 mmol) was dissolved in OEt_2 (3 mL), and *t*-BuNC (3.5 mL, 0.0309 mmol, 0.97 equiv) was added, eliciting a rapid color change to dark red-brown. ^{2}H NMR analysis of the reaction mixture showed a peak at 11.1 ppm corresponding to the adduct Mo(CN-*t*-Bu)(N[R]Ar)$_3$.

4.25. Reaction of Mo(N[R]Ar)$_3$ with *t*-BuNCO. Mo(N[R]Ar)$_3$ (0.0217 g, 0.0338 mmol) was dissolved in *t*-BuNCO (0.75 g), and the reaction mixture was stirred for 24 h. Examination of the reaction mixture by ^{2}H NMR showed Mo(N[R]Ar)$_3$ (δ = 64.7), paramagnetic material (δ = 29.4 and 26.4), (Mo(CN-*t*-Bu)(N[R]Ar)$_3$ (δ = 11.6), Mo(O)(N[R]Ar)$_3$ (δ = 7.8), and diamagnetic material (δ = 2.9−3) in a 60:1:5:1:3:10 ratio.

4.26. Reaction of Mo(N[R]Ar)$_3$ with O$_2$SMe$_2$. Mo(N[R]Ar)$_3$ (0.0211g, 0.0328 mmol) was dissolved in THF (2 mL) and O$_2$SMe$_2$ (0.0030 g, 0.0319 mmol, 0.97 equiv) was added. The reaction mixture was stirred for 48 h, at which point it was examined by ^{2}H NMR, showing Mo(N[R]Ar)$_3$ (δ = 64.3) and diamagnetic material (δ = 2.2−1.8) in a 5:1 ratio, along with a tiny amount of Mo(O)(N[R]Ar)$_3$ (δ = 7.5).

4.27. Reaction of Mo(O)(N[R]Ar)$_3$ with PPh$_3$. Mo(O)(N[R]Ar)$_3$ (0.0480 g, 0.0729 mmol) was dissolved in toluene, and PPh$_3$ (0.0400 g, 0.153 mmol, 2.1 equiv) was added. The reaction was stirred for 24 h, at which point examination by ^{2}H NMR showed only the starting oxo complex. Examination of the reaction by ^{31}P NMR showed only PPh$_3$ (δ = −4.41).

4.28. Reaction of Mo(O)(N[R]Ar)$_3$ with OSMe$_2$. Mo(O)(N[R]-Ar)$_3$ (0.0312 g, 0.0474 mmol) was dissolved in OEt$_2$ (5 mL), and OSMe$_2$ (8.5 mL, 0.12 mmol, 2.5 equiv) was added. The reaction was stirred for 20 h, at which point it was examined by ^{2}H NMR, showing the presence of a significant amount of starting oxo complex. The reaction mixture was stirred an additional 48 h, at which point the reaction solution was red-brown. Analysis of the reaction mixture by ^{1}H NMR showed H(N[R]Ar) and Mo(O)$_2$(N[R]Ar)$_2$ in a 3.5:1 ratio.

4.29. Reaction of Mo(N[R]Ar)$_3$ with O$_2$. Mo(N[R]Ar)$_3$ (0.2200 g, 0.3422 mmol) was dissolved in OEt$_2$ (10 mL), and O$_2$ (8.5 mL, 0.35 mmol, 1.0 equiv) was added slowly over a 2 min period. The solution became dark blue for about 10 s and then turned green. After 30 s, the solution was dark brown. ^{2}H NMR at this point showed the presence of one part Mo(O)(N[R]Ar)$_3$ and two parts diamagnetic material. ^{1}H NMR spectra of the material showed five products: Mo(O)$_2$(N[R]Ar)$_2$ H(N[R]Ar), two unidentified products, and Mo(O)-(N[R]Ar)$_3$ in a 2:1:1:1 ratio.

4.30. Thermolysis of Mo(O)(NAr)(N[R]Ar)$_2$. Mo(O)(NAr)(N[R]-Ar)$_2$ (ca. 0.015 g) was dissolved in C$_6$D$_6$ (ca. 1 mL) and sealed in an NMR tube. The mixture was heated at 110 °C for 82 h, at which point it appeared to contain three products, Mo(O)$_2$(N[R]Ar)$_2$, Mo(O)(NAr)-(N[R]Ar)$_2$, and an unknown product, presumably Mo(NAr)$_2$(N[R]Ar)$_2$, in a 1:2:1 ratio.

4.31. Reaction of Mo(O)(NAr)(N[R]Ar)$_2$ with Benzaldehyde. Mo(O)(NAr)(N[R]Ar)$_2$ (0.0471 g, 0.0788 mmol) and benzaldehyde (0.080 mL, 0.787 mmol, 10 equiv) were dissolved in OEt$_2$ (3 mL) and stirred at room temperature for 72 h. ^{1}H NMR showed primarily starting material and peaks due to Mo(O)$_2$(N[R]Ar)$_2$ and Ph(H)C═NAr.

4.32. Thermodynamic Measurements. 4.32.1. General Considerations. All manipulations involving molybdenum complexes were performed under inert atmospheres of argon in a Vacuum Atmospheres glovebox containing less than 1 ppm oxygen and water. Calorimetric measurements were performed using a Calvet calorimeter (Setaram C-80) which was periodically calibrated by the TRIS reaction[55] or the enthalpy of solution of KCl in water.[56] The experimentally determined enthalpies for these two standard calibration reactions are the same within experimental error to literature values. This calorimeter has been previously described,[57] and typical procedures are described below. Experimental enthalpy data are reported with 95% confidence limits.

4.32.2. ^{2}H NMR Titrations. Prior to the calorimetric experiments, an accurately weighed amount (±0.1 mg) of the molybdenum complex was placed in an NMR tube, and toluene was subsequently added. The solution was titrated with a large excess of the reagent of interest. The reactions were monitored by ^{2}H NMR spectroscopy, and the reactions were found to be rapid, clean, and quantitative under experimental calorimetric conditions. These conditions are necessary for accurate and meaningful calorimetric results and were satisfied for the molybdenum reactions investigated with ONC$_5$H$_5$ and ethylene sulfide. Only reactants and products were observed in the course of the NMR titration.

4.32.3. Calorimetric Measurement for Reaction Between Mo(N[R]Ar)$_3$ and ONC$_5$H$_5$. The mixing vessels of the Setaram C-80 were cleaned, dried in an oven maintained at 120 °C, and then taken into the glovebox. A 20−30 mg sample of Mo(N[R]Ar)$_3$ was accurately weighed into the lower vessel; the vessel was closed and sealed with 1.5 mL of mercury. Four milliliters of a 25% stock solution of ONC$_5$H$_5$ [0.5 g of pyridine *N*-oxide in 25 mL of toluene] was added, and the remainder of the cell was assembled, removed from the glovebox, and inserted in the calorimeter. The reference vessel was loaded in an identical fashion with the exception that no organomolybdenum complex was added to the lower vessel.

After the calorimeter had reached thermal equilibrium at 30.0 °C (about 1.5 h), the calorimeter was inverted thereby allowing the reactants to mix. After reaching thermal equilibrium, the vessels were removed from the calorimeter, taken into the glovebox, opened, and analyzed using ^{1}H NMR spectroscopy. Conversion to Mo(O)(N[R]Ar)$_3$ was found to be quantitative under these reaction conditions. The enthalpy of reaction, −74.6 ± 1.2 kcal mol^{-1}, represents the average of five individual calorimetric determinations. The enthalpy of solution of Mo(N[R]Ar)$_3$ was then added to this value to obtain a value of −83.5 ± 1.4 kcal mol^{-1} for all species in solution.

4.32.4. Calorimetric Measurement for Reaction between Mo(N[R]Ar)$_3$ and Ethylene Sulfide. The mixing vessels of the Setaram C-80 were cleaned, dried in an oven maintained at 120 °C, and then taken into the glovebox. A 20−30 mg sample of Mo(N[R]Ar)$_3$ was accurately weighed into the lower vessel; the vessel was closed and sealed with 1.5 mL of mercury. Four milliliters of a 25% stock solution of ethylene sulfide [0.5 g of ethylene sulfide in 25 mL of toluene] was added, and the remainder of the cell was assembled, removed from the glovebox, and inserted in the calorimeter. The reference vessel was loaded in an identical fashion with the exception that no organomolybdenum complex was added to the lower vessel.

After the calorimeter had reached thermal equilibrium at 30.0 °C (about 1.5 h), the calorimeter was inverted thereby allowing the reactants to mix. After reaching thermal equilibrium, the vessels were removed from the calorimeter, taken into the glovebox, opened, and analyzed using ^{1}H NMR spectroscopy. Conversion to Mo(S)(N[R]Ar)$_3$ was found to be quantitative under these reaction conditions. The enthalpy of reaction, −36.3 ± 1.2 kcal mol^{-1}, represents the average of five individual calorimetric determinations. The enthalpy of solution of Mo(N[R]Ar)$_3$ was then added to this value to obtain a value of −45.2 ± 1.2 kcal mol^{-1} for all species in solution.

4.32.5. Calorimetric Measurement of Enthalpy of Solution of Mo(N[R]Ar)$_3$. In order to consider all species in solution, the enthalpy of solution of Mo(N[R]Ar)$_3$ had to be directly measured in the solvents utilized. This was performed by using a similar procedure as the one described above with the exception that no reagent was added to the reaction cell. This enthalpy of solution represents the average of three individual determinations and is 8.9 ± 0.2 kcal mol^{-1} in toluene.

4.33. X-ray Structure of Mo(O)(N[R]Ar)$_3$. A black needle of approximate dimensions 0.8 × 0.5 × 0.2 mm was obtained from a chilled OEt$_2$ solution. The crystal was mounted on a glass fiber. Data collection was carried out on a Siemens Platform goniometer with a CCD detector. The total data collected were 7169 reflections ($-10 \le h \le 10$, $-11 \le k \le 10$, $-22 \le l \le 21$), of which 4915 were unique (R_{int} = 0.0309). Semiempirical corrections from ψ-scans were applied. The structure was solved by direct methods (SHELXTL V5.0, G. M. Sheldrick and Siemens Industrial Automation, Inc., 1995) in conjunction with standard difference Fourier techniques. All non-hydrogen atoms were refined anisotropically, and hydrogen atoms were placed in calculated (d(C−H) = 0.96 Å) positions. The residual peak and hole electron density were 0.446 and −0.558 e Å^{-3}. Tables of positional and thermal parameters for the structure of Mo(O)(N[R]Ar)$_3$ have already appeared in print.[53] Crystal and refinement data: formula = C$_{36}$H$_{54}$MoN$_3$O, space group $P\bar{1}$, a = 9.8974(12), b = 9.9883(14), and c = 20.254(2) Å, α = 95.745(10)°, β = 92.324(8)°, γ = 117.356(8)°, Z = 2, U = 1760.9(4) Å^3, D_{calcd} = 1.208 g cm^{-3}, 188 K, radiation Mo Kα, λ = 0.710 73 Å, μ(Mo Kα) = 0.402 mm^{-1}, F(000) = 682, total reflections = 7169, independent reflections = 4915, data/

(55) Ojelund, G. W. I. *Acta Chem. Scand.* **1968**, *22*, 1691.
(56) Kilday, M. V. *J. Res. Natl. Bur. Stand. (U.S.)* **1980**, *85*, 467.
(57) Nolan, S. P.; Hoff, C. D. *J. Organomet. Chem.* **1985**, *282*, 357.

Table 1. Crystal and Refinement Data for the Isomorphic $Mo(E)(N[R]Ar)_3$ (E = S, Se, and Te) Complexes

	E		
	S	Se	Te
space group	$P2_1/c$	$P2_1/c$	$P2_1/c$
a (Å)	13.9099(8)	13.9372(7)	14.108(2)
b (Å)	12.8972(8)	12.8821(7)	12.762(3)
c (Å)	19.9860(12)	19.9510(10)	20.083(4)
β (deg)	93.0580(10)	92.9060(10)	92.558(11)
Z	4	4	4
U(Å^3)	3580.4(4)	3577.4(3)	3612.2(13)
D_{calcd} (g cm^{-3})	1.219	1.307	1.383
T (K)	188(2)	159(2)	161(2)
radiation	Mo-Kα	Mo-Kα	Mo-Kα
λ(Å)	0.71073	0.71073	0.71073
μ(Mo Kα) (mm^{-1})	0.451	1.411	1.181
F(000)	1396	1468	1540
total reflections	13213	12674	14461
independent reflections	5098	5075	5182
data/parameter ratio	5093/371	5073/370	5180/371
R_1	0.0527	0.0391	0.0256
wR_2	0.1015	0.0976	0.0634
GOF	1.168	1.285	1.008

parameter ratio = 4915/370, $R_1 = 0.0341$, $wR_2 = 0.0959$, GOF = 1.053, residuals based on $I > 2\sigma(I)$.

4.34. X-ray Structures of the Isomorphic $Mo(E)(N[R]Ar)_3$ (E = S, Se, and Te) Complexes. $Mo(S)(N[R]Ar)_3$: A black needle of approximate dimensions 0.55 × 0.23 × 0.11 mm was obtained from a chilled OEt_2 solution. The crystal was mounted on a glass fiber. Data collection was carried out on a Siemens Platform goniometer with a CCD detector. The limiting indices were $-15 \le h \le 15$, $-14 \le k \le 7$, $-22 \le l \le 22$. No absorption corrections were applied. The structure was solved by direct methods (SHELXTL V5.0, G. M. Sheldrick and Siemens Industrual Automation, Inc., 1995) in conjunction with standard difference Fourier techniques. Least-squares refinement was based upon F^2. All non-hydrogen atoms were refined anisotropically, and hydrogen atoms were placed in calculated positions. The residual peak and hole electron density were 0.376 and −0.709 e Å^{-3}. See Table 1 for crystal and refinement data for the $Mo(E)(N[R]Ar)_3$ (E = S, Se, and Te) complexes. Tables of positional and thermal parameters for the structures of $Mo(E)(N[R]Ar)_3$ (E = S, Se, and Te) have already appeared in print.[53]

$Mo(Se)(N[R]Ar)_3$: A black needle of approximate dimensions 0.75 × 0.32 × 0.22 mm was obtained from a chilled OEt_2 solution. Data collection was as for $Mo(S)(N[R]Ar)_3$ and the limiting indices were: $-7 \le h \le 15$, $-14 \le k \le 14$, $-22 \le l \le 15$. A semiempirical absorption correction from ψ-scans was applied. Structure solution and refinement was as that for $Mo(S)(N[R]Ar)_3$. All non-hydrogen atoms were refined anisotropically, and hydrogen atoms were placed in calculated positions. The residual peak and hole electron density were 0.394 and −0.501 e Å^{-3}.

$Mo(Te)(N[R]Ar)_3$: A black needle of approximate dimensions 0.65 × 0.48 × 0.23 mm was obtained from a chilled OEt_2 solution. The crystal was mounted on a glass fiber. Data collection was as that for $Mo(S)(N[R]Ar)_3$, and the limiting indices were $-12 \le h \le 15$, $-14 \le k \le 11$, and $-22 \le l \le 22$. No absorption corrections were applied. Structure solution and refinement was as for $Mo(S)(N[R]Ar)_3$. All non-hydrogen atoms were refined anisotropically, and hydrogen atoms were placed in calculated positions. The residual peak and hole electron density were 0.399 and −0.359 e Å^{-3}.

4.35. X-ray Structure of $(\mu$-CS)$[Mo(N[R]Ar)_3]_2\cdot(OEt_2)_2$. A greenish brown needle of approximate dimensions 0.40 × 0.21 × 0.18 mm was obtained from a chilled OEt_2 solution. The crystal was mounted on a glass fiber. Data collection was carried out on a Siemens Platform goniometer with a CCD detector at 188 K using Mo Kα radiation (λ = 0.710 73 Å). The total data collected were 11 885 reflections ($-16 \le h \le 13$, $-16 \le k \le 12$, $-22 \le l \le 20$), of which 7493 were unique ($R_{int} = 0.0673$). Semiempirical corrections from ψ-scans were applied. Structure solution and refinement was as that for $Mo(S)(N[R]Ar)_3$. Least-squares refinement based upon F^2 converged with residuals of $R_1 = 0.1035$, $wR_2 = 0.2107$, and GOF = 1.209 based upon $I > 2\sigma(I)$. All non-hydrogen atoms were refined anisotropically, with the exception of the two disordered OEt_2 molecules and a disordered *tert*-butyl group; hydrogen atoms were placed in calculated positions. The residual peak and hole electron density were 0.920 and −0.512 e Å^{-3}. Tables of positional and thermal parameters for the structure of $(\mu$-CS)$[Mo(N[R]Ar)_3]_2$ have already appeared in print.[53] Crystal data: triclinic, a = 14.6441(3), b = 15.2700(2), and c = 20.5956(4) Å, V = 4150.44(13) Å^3, α = 89.1990(10)°, β = 77.8370(10)°, γ = 67.6530(10)°, space group $P\bar{1}$, $Z = 2$, $\mu = 0.372$ mm^{-1}, $M_r = 1432.76$ for $C_{81}H_{119}Mo_2N_6O_2S$, $D_{calcd} = 1.146$ g cm^{-3}, and $F(000) = 1526$.

Acknowledgment. For financial support of this work C.C.C. thanks the National Science Foundation (CAREER Award CHE-9501992), DuPont (Young Professor Award), the Packard Foundation (Packard Foundation Fellowship), Union Carbide (Innovation Recognition Award), and 3M (Innovation Fund Award). C.C.C. is a Sloan Foundation Fellow (1997−2000). Thermochemical studies were supported by a grant (NSF-9631611) from the National Science Foundation. The use of computation facilities and programs at the Emerson Center is acknowledged.

Supporting Information Available: Tables of positional and thermal parameters for the crystal structures of $Mo(E)(N[R]Ar)_3$ (E = O, S, Se, and Te) and $(\mu$-CS)$[Mo(N[R]Ar)_3]_2\cdot(OEt_2)_2$ (7 pages). An X-ray crystallographic file, in CIF format, is available through the Web only. See any current masthead page for ordering information and Web access instructions.

JA971491Z